Summer 7-22-2022

Construction and Operation of a Pilot-Scale Odor Control Device

Brendan Bunker
University of Nebraska-Lincoln, brendan.bunker23@gmail.com

CONSTRUCTION AND OPERATION OF A PILOT-SCALE ODOR CONTROL DEVICE

by

Brendan Bunker

A THESIS

Presented to the Faculty of

The Graduate College at the University of Nebraska

In Partial Fulfillment of Requirements

For the Degree of Master of Science

Major: Environmental Engineering

Under the Supervision of Professors Bruce Dvorak and Ashraf Aly Hassan

Lincoln, Nebraska

July 2022

CONSTRUCTION AND OPERATION OF A PILOT-SCALE ODOR CONTROL DEVICE

Brendan Bunker, M.S.

University of Nebraska, 2022

Advisors: Bruce I. Dvorak and Ashraf Aly Hassan

Hydrogen sulfide (H_2S) is a naturally occurring by-product of anaerobic digestion and causes an odor that can be a nuisance and a public health risk at higher concentrations. This compound can be treated through various means, but one of particular interest is a biotrickling filter (BTF). Such devices have excellent H_2S treatment efficiencies, but start-up costs can be steep. The primary goal of this study is to explain the design and operation of a low-cost odor control device for improving environmental air quality in Nebraska using a BTF. This device has the potential for application as a preliminary step in treating impurities in methane-rich gas and for treating other volatile organic compounds (VOCs) with the goal of reducing treatment costs and overall footprint. Preliminary experiments were completed to investigate cyclic adsorption and thermal regeneration of H_2S from granular activated carbon (GAC), a foundational component of the device. Results from these experiments demonstrated the effectiveness of this concept; virgin samples carbon were regenerated at approximately 70% efficiency, with subsequent cycles showing roughly 50% efficiency. The pilot device was installed at the Loup Central Landfill and operated for three months. Gas emitted from the leachate cleanout system was sampled for H_2S, but none was detected despite positive results from samples taken during the previous year. The gas was supplemented with manufactured H_2S during experimentation. Data from the landfill site provided evidence that gas containing H_2S was successfully captured and concentrated via GAC columns. The activated carbon captured incoming H_2S at an efficiency of

roughly 75% (± 15%) and regenerated at an overall efficiency of 76% (± 26%), noting that multiple cycles produced regeneration above 100%. Results from the BTF initially showed signs of degradation, and prolonged operation showed that it did not efficiently treat H_2S. Despite limited biological treatment, the pilot odor control device produced successful results in other facets. Some recommended changes to the pilot device and its operation appear following an explanation of the experimental results.

AUTHOR'S ACKNOWLEDGEMENTS

The work described in this thesis would not have been possible without the help of many mentors and colleagues.

I would like to thank my faculty advisors, Dr. Dvorak and Dr. Aly Hassan, for their guidance and help. Collaborating with them over the past couple years has been a joy. I'd like to also extend my gratitude to Dr. Xu Li and Dr. Hunter Flodman for serving on my thesis committee.

Thank you to Katie Mowat, Andrew Donesky, Andrew Hansen, Aaron Evans, Paul Marxhausen, Dr. David Admiraal, and Peter Hilsabeck for their assistance and advice during the construction and operation of the pilot odor control device. Their help was invaluable as I pieced this project together.

I would also like to thank Jeff Selden and his staff at the Loup Central Landfill. This project would not have succeeded without the support they provided before, during, and after the operating stage at the landfill site.

Finally, I would like to thank my wife, my parents, and the rest of my family for their help and support during my academic journey.

GRANT INFORMATION

Funding for this work was provided by:

The Nebraska Environmental Trust

Project Number 19-159-2, Low-Cost Biological Odor Treatment Using an Adsorption/Desorption Concentrator Unit for Reducing Sulfur Emission in Nebraska.

TABLE OF CONTENTS

TABLE OF TABLES

TABLE OF FIGURES

CHAPTER 1: INTRODUCTION

1.1. Landfills and Odor Problems

In 2018, landfills in the United States received approximately 146.1 million tons of municipal solid waste (US EPA 2017). As this waste decomposes, it produces odors that can become a nuisance to those living nearby. Odors emitted from landfills may cause temporary ailments such as headaches and nausea, especially for susceptible persons with respiratory ailments who may be sensitive to chemical compounds in the air (Tansel and Inanloo 2019). The primary contributors to the offensive smell in landfill gas are ammonia and hydrogen sulfide (H_2S). Ammonia produces a strong, pungent odor while H_2S produces a smell like rotten eggs. The main components of anaerobic landfill gas include carbon dioxide and methane, each contributing roughly 40 – 60% to the total volume (Omar and Rohani 2015). The odor-producing compounds ammonia and hydrogen sulfide each typically make up less than 1% of the gas volume. Even in small concentrations, these compounds become an issue because of their low odor thresholds.

Regulative requirements may prompt the treatment of landfill gas emissions. Even if a specific compound is not explicitly regulated, it may still require removal because of odor complaints or health and safety concerns. To address these issues, the gas must first be captured, either from cleanout wells or from fugitive emissions, and then treated. In some instances, landfill gas can be collected and used in applications such as power generation if it contains a sufficient volume of methane. Landfills that do not capture landfill gas for such uses may treat it using various methods, including combustion, non-combustion technologies, and odor-control procedures. It is common for landfills that are

focused on controlling odors to employ one of three primary types of systems: biochemical systems, chemical systems, or physical systems.

Physical and chemical techniques have been broadly implemented because of their consolidated experience in design and operation, but also because of their quick start-up and low empty bed residence times that allow for more compact equipment (Alfonsín et al. 2015). Systems that employ these technologies typically also have higher suitability for the treatment of high concentrations of pollutants. Biochemical or biological treatment techniques have become more widely used as research has shown similar odor removal efficiencies as conventional methods (Gospodarek et al. 2019). Biological treatment is more environmentally friendly than physical and chemical methods and does not require the addition of chemicals. Methods that utilize this treatment strategy can be operated at normal temperatures and atmospheric pressure, which allows for simple process management. The primary mechanism for removal in biological treatment is microbial degradation which is usually oxidative and produces safe end-products, such as carbon dioxide, water, nitrates, and sulfates.

H_2S can be successfully treated with the previously mentioned biological methods. These methods are commonly divided into biofilters, bioscrubbers, and biotrickling filters (BTFs) (Gabriel and Deshusses 2003). The performance of these technologies varies based on several factors including the effectiveness of the microbial population responsible for degradation, pollutant loading rates, and gas contact times. Nonetheless, these biotechnologies demonstrate removal efficiencies that rival common physical/chemical treatments.

At present, this thesis will consider the treatment of H_2S using a BTF. The primary drawback of treating H_2S with a BTF is the large footprint required for installation, start-up, and sustained operation. For process streams with a smaller volume of H_2S emissions, this suggests that BTFs may not be as cost-effective as a physical or chemical treatment method. A large reactor volume would be required even for small-scale operation. Furthermore, concentration of the air stream containing H_2S emissions may provide a reduction of direct and operating costs of a BTF by minimizing the required reactor volume.

The use of granular activated carbon (GAC) together with a BTF may provide a method for concentrating gas containing H_2S for further treatment in a biological system. Its high porosity, extensive surface area, and low cost make it an attractive choice (Coppola and Papurello 2019; Marsh and Reinoso 2006). H_2S in air emissions has been effectively captured by GAC in many instances. Once captured, H_2S can be removed by thermal regeneration which would, in theory, produce gas that is more concentrated than the gas that first encountered it. Confirmation of the feasibility of this concept and its implementation serve as the basis for this study.

1.3. Goals and Objectives

The main goal of this study is to build and operate an odor control device at Loup Central Landfill to demonstrate a novel technology resulting in a reduction in cost and volume of the required treatment device. In addition, a series of experiments must be conducted to investigate the feasibility of using GAC to concentrate odorous gas containing H_2S. The specific objectives include the determination of the adsorption and

desorption kinetics of GAC, designing and building the odor control device, and operating the device at the Loup Central Landfill.

1.4. Organization of Thesis

The topics described in this work are summarized in Figure 1.1 shown below. The first chapter of the thesis has introduced some of the primary topics to provide context for the pilot odor control device. The next chapter, Chapter 2 will consider similar topics in more depth by way of a literature review. Chapter 3 will explain the experiments that were conducted as a precursor to the construction and operation of the pilot odor control device. Specifically, these experiments investigated cyclic adsorption and desorption of H_2S from samples of GAC. Chapter 4 will detail the work that was done to investigate the test site and Chapter 5 will describe the experiments and the results that were obtained from operations at the landfill. The final chapter will review the findings of the previous chapters and reflect on future work. Additionally, there will be several appendices that will give further information related to the pilot odor control device, its operation, and its construction. A diagram which summarizes the layout of this thesis appears below (Figure 1.1.)

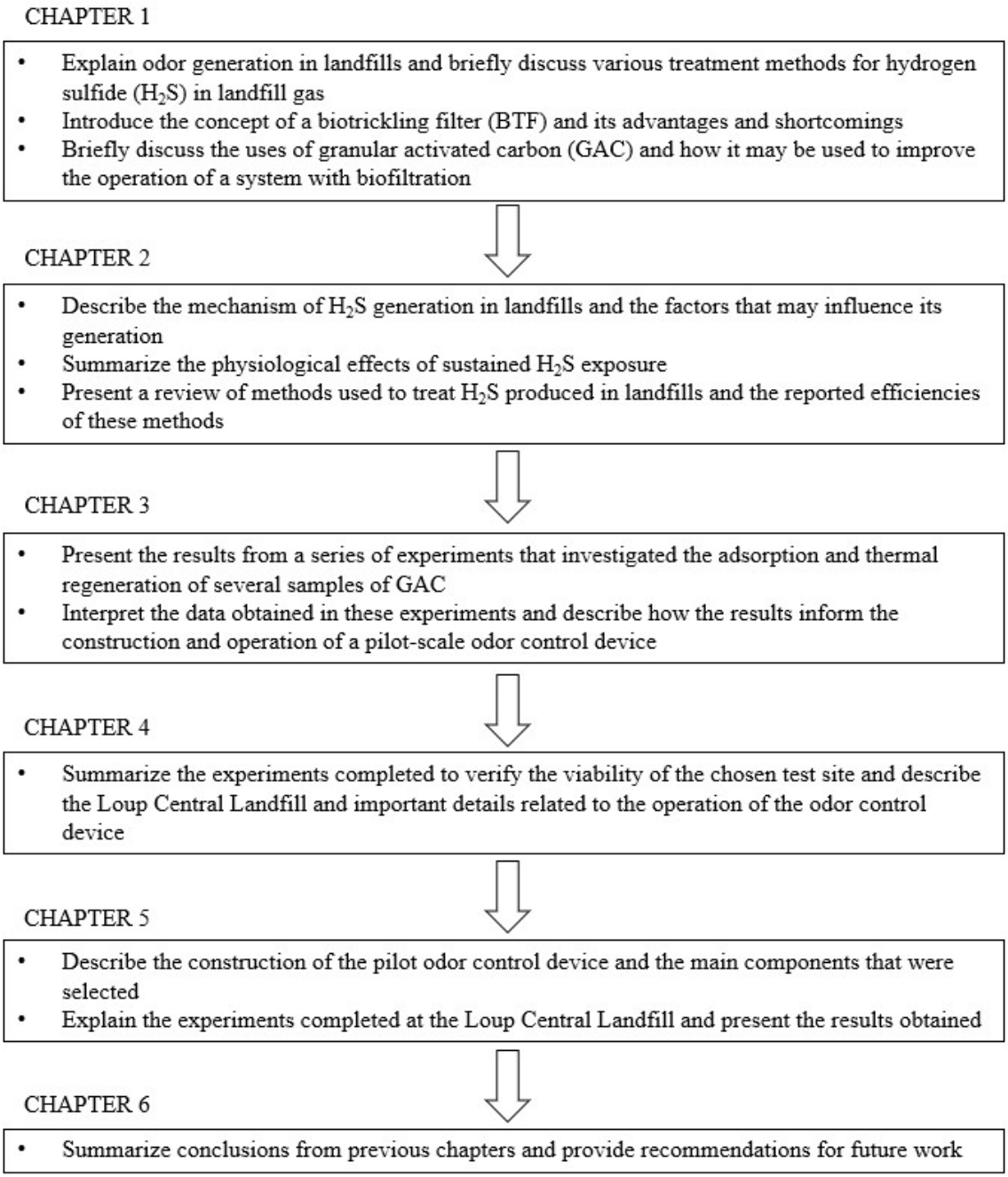

Figure 1.1: Organization of Thesis

CHAPTER 2: LITERATURE REVIEW

2.1. Introduction

This chapter contains a discussion of topics relevant to the treatment of odors caused by H_2S and the principles utilized to construct and operate the pilot odor control device. Specifically, the physical-chemical and biological treatment of odors caused by H_2S will be discussed as they pertain to the inner workings of the pilot odor control device, which will be explained in later chapters.

2.2. H_2S Generation in Landfills

Hydrogen sulfide (H_2S) is an odorous compound commonly identified in landfills, wastewater treatment plants, and sewers (Al Mamun 2015; Letelier-Gordo et al. 2020). Along with methyl mercaptan (CH_3SH), dimethyl sulfide ($(CH_3)_2S$), and ammonia (NH_3), H_2S has been identified as a major contributor to the odors caused by landfills (Ko et al. 2015). One explanation for why H_2S can cause such potent odors is its low odor threshold. H_2S can be detected by human olfactory senses at concentrations as low as 0.4 parts per billion (ppb) (NAGATA 1990) and produces a characteristic "rotten-egg" smell. For this reason, odor complaints associated with H_2S emissions are common depending on atmospheric conditions (Xu and Townsend 2014). To attain a comprehensive understanding of the generation of H_2S from landfills, a review of the mechanisms, causes, and main factors related to this topic is necessary.

2.2.1. Source of Sulfur in Landfills

H_2S is produced in landfills by the reduction of elemental sulfur to H_2S by sulfate-reducing bacteria (SRB). SRB are microorganisms that, in the absence of oxygen, use sulfate (SO_4^{2-}) as an electron acceptor for the degradation of organic compounds (Muyzer

and Stams 2008). SRB can be found almost anywhere there is enough sulfur, but are particularly abundant in sewers, wastewater systems, and landfills (Ko et al. 2015). Competition exists between SRB and methanogenic bacteria because they consume a common substrate. Methanogenic bacteria are responsible for the formation of methane and are often outcompeted by SRB (Kristjansson and Schönheit 1983). Nonetheless, both methane and hydrogen sulfide are commonly found in landfill gas in particular because of a symbiotic relationship that exists between the bacteria that produces them (Kushkevych et al. 2017).

One of the main contributors to the elemental sulfur in landfills is gypsum ($CaSO_4 \cdot 2H_2O$) which is abundant in drywall and typically disposed of in construction and demolition (C&D) landfills (Lee et al. 2006). Gypsum is a mineral composed of calcium sulfate ($CaSO_4$) and water and is widely used for interior walls because of its resistance to fire. Although it is easily recyclable in many places, it is commonly landfilled (Weimann et al. 2021). Depending on the location, gypsum drywall can make up as much as 12% of the total waste in a landfill (Zhang et al. 2017). Other contributors to sulfur in landfills include food waste, paper waste, and wastewater sludge, which is commonly disposed of after dewatering (Ko et al. 2015).

Several factors can influence the growth of SRB in landfills. One of the most important is moisture content. A common strategy for mitigating odors due to H_2S is reducing the amount of infiltrating rainwater (Zhang et al. 2014). The reduction of moisture increases the amount of air that migrates into landfills, thereby reducing H_2S production. Furthermore, the presence of moisture content in the cover soil may also reduce H_2S emission rates. Findings from one study suggested that while the

concentration of H_2S underneath cover soil remained similar before and after a rain event, emissions dropped when cover soil was wet and increased when it was dry (Xu and Townsend 2014).

Another important that may influence the emission of H_2S is temperature. It is well-known that microbial activity decreases when temperatures drop. In agreement with this fact, H_2S emissions have been found to decline when ambient temperatures are cooler (Hu et al. 2017). The pH of the surrounding environment can also play an important role in the growth of SRB. SRB tends to fare better in a neutral pH environment (O'Flaherty et al. 1998). Decreasing the pH below 5 or raising it to above 9 suppresses the growth of SRB (Gutierrez et al. 2009; Kushkevych et al. 2017).

Finally, as mentioned previously, SRB thrives in environments free from oxygen. For this reason, air venting has been shown to produce a significant drop in H_2S production (Zhang et al. 2014). These findings agree with the knowledge that SRB is most productive in anaerobic conditions.

2.2.2. Levels of H_2S in Landfills

A variety of methods exist for measuring the concentration of H_2S emitted from landfills. In particular, measurements can be reported as concentrations in ambient air surrounding a landfill, in landfill gas samples, or as flux rates from landfill surfaces (Ko et al. 2015). Data collected using only one technique most likely does not accurately describe the whole of H_2S emissions from a landfill because levels of H_2S may vary with techniques and different sampling points. Nonetheless, a large body of measured H_2S concentration data in landfill environments.

Depending on the technique and location, concentrations of H_2S may appear within a large range of values. Typically, concentrations are much lower in samples taken from ambient air because they are further removed from the emission source. One study showed a range of values between 40 and 370 ppb at six sampling points surrounding the landfill (Ying et al, 2012). Concentrations can be much higher in landfill gas, sometimes ranging between 0.003 – 12,000 parts per million (ppm) (Lee et al, 2006). Finally, flux rates of H_2S measured at the surface of the landfill can be on the order of 0.2 – 1.8 mg/m^2-d (Eun et al. 2007).

2.2.3. Health Effects

In addition to causing odors, exposure to H_2S may also cause health issues. The harm that H_2S can cause depend on the duration, frequency, and concentration of the exposure. A detailed summary of the pathophysiological response to various concentrations of H_2S is shown below (Table 2.1). Even at lower concentrations, exposure to H_2S over long periods can result in unpleasant health effects.

2.3. Treatment of Odors Caused by H_2S

As concern around the H_2S emissions from landfills has grown in recent years, so has the interest in methods for treating it. When the presence of odors caused by H_2S is confirmed, authorities may dictate some form of remediation. There are numerous processes for addressing this issue, but they can be grouped into one of two primary approaches. Depending on the situation, either the generation of H_2S is inhibited, or H_2S is removed from the gas that is emitted. Methods used to carry out either of these two approaches will be discussed subsequently.

Table 2.1: Human responses to various concentrations of H_2S in the air (Rubright et al., 2017).

Concentration (ppm)	**Expected Effects/Symptoms**
0.00011 – 0.00033	Typical background concentrations (OSHA)
0.0004	Lowest concentration detectable by human olfactory senses
0.01 – 1.5	Odor threshold. Odor becomes more offensive at 3–5 ppm. Above 30 ppm, odor described as sweet or sickeningly sweet (OSHA)
2 – 5	Prolonged exposure may cause nausea, tearing of the eyes, headaches, or loss of sleep. Airway problems (bronchial constriction) in some asthma patients (OSHA).
20	Possible fatigue, loss of appetite, headache, irritability, poor memory, and dizziness (OSHA).
50 – 100	Slight conjunctivitis and respiratory tract irritation after 1-hour exposure may cause digestive upset and loss of appetite (ANSI and OSHA).
100	Coughing, eye irritation, loss of sense of smell after 2–15 minutes. Altered respiration, pain in the eyes, and drowsiness after 15–30 minutes followed by throat irritation after 1 hour. (ANSI and OSHA).
100-150	Loss of smell (olfactory fatigue or paralysis) (OSHA).
200-300	Marked conjunctivitis and respiratory tract irritation after 1 hour of exposure (ANSI and OSHA). Pulmonary edema may occur from prolonged exposure (OSHA)
500-700	Staggering, collapse in 5 minutes (OSHA). Serious damage to the eyes. Loss of consciousness and possibly death in 30 minutes - 1 hour (ANSI and OSHA)
700-1000	Rapid unconsciousness, " knockdown" or immediate collapse within 1 to 2 breaths, cessation of respiration, and death within minutes (ANSI, ATSDR, and OSHA).
1000-2000	Unconsciousness at once, with early cessation of respiration and death in a few minutes. Death may occur even if the individual is removed to fresh air at once (ANSI and OSHA).
Abbreviations: ANSI, American National Standards Institute; ATSDR, Agency for Toxic Substances and Disease Registry; OSHA, Occupational Safety and Health Administration.	

2.3.1. Inhibition of H_2S Generation

The simplest way to prevent the production of H_2S is by removing the source of substrate for SRB. The removal of sulfur-containing materials such as gypsum drywall would reduce the activity of SRB in landfills. Inhibitors can also be added to achieve the same effect. The type of inhibitor used depends largely on the waste composition and type of SRB present but may include chemical additives such as sodium molybdate (Na_2MoO_4), ferric chloride ($FeCl_3$), and hydrated lime ($Ca(OH)_2$) (Xu et al. 2011). The growth of competing anaerobic bacteria, such as nitrate-reducing bacteria (NRB), may also be an effective method of inhibiting SRB activity (Greene et al. 2003).

2.3.2. Removal of H_2S from Landfill Gas

H_2S can be effectively removed from landfill gas after capturing it, or by treating it directly as fugitive gas. Various technologies exist for each approach. The removal of H_2S from captured landfill gas has been accomplished through a variety of physicochemical and biological means (Burgess et al. 2001). The physicochemical treatment of H_2S contains a range of treatment processes including absorption (Rasi et al. 2014), adsorption (He et al. 2011), chemical scrubbers, thermal oxidation, and catalytic oxidation. Many of these methods have been well-developed and commercially adopted (Georgiadis et al. 2020). They commonly require the addition of chemicals in addition to substantial energy expenditure (Omar and Rohani 2015). In contrast, the biological treatment of H_2S relies on the growth of microbial populations to degrade pollutants and produce mostly carbon dioxide, water, sulfates, and nitrates. This type of treatment has received much attention and is widely accepted as an advantageous method for removing H_2S from gas streams (Barbusiński et al. 2021). Its benefits include a relatively low

carbon footprint, excellent removal efficiencies of H_2S, and low operating costs (Federation 2020). The degradation mechanism of this treatment method is an oxidative reaction that converts H_2S to SO_4^{2-}. Additionally, H_2S is used as an energy source by bacteria that require carbon dioxide or dissolved carbonate as a carbon source. There are several sulfur species that may be produced during this process, including S^0, $S_2O_3^{2-}$, and SO_3^{2-}. (Kim and Deshusses 2005).

The primary biological technologies used for H_2S treatment are biofilters (Yang and Allen 1994), bioscrubbers (Haosagul et al. 2020; San-Valero et al. 2019), and BTFs (Gabriel and Deshusses 2003). The performance of these technologies varies based on many factors, including the effectiveness of the microbial population responsible for degradation, pollutant loading rates, and gas contact times. Nonetheless, these biotechnologies generally demonstrate excellent removal efficiencies. A laboratory-scale biofilter study reported removal efficiencies greater than 99 percent for H_2S inlet concentrations ranging between 5 and 2650 ppmv (Yang and Allen 1994). This system contained various types of yard waste compost as filter material. Additionally, a fixed film bioscrubber study that utilized a mixture of two strains of bacteria, Acinetobacter sp. MU1_03 and A. faecalis MU2_03, achieved 98 percent H_2S removal of an inlet gas stream with 100 ppm_v (Potivichayanon et al. 2006). Finally, a full-scale BTF study demonstrated H_2S removal rates exceeding 95 percent for H_2S concentrations as high as 30 ppm_v (Gabriel and Deshusses 2003). Efficiencies of approximately 90 percent were recorded for inlet concentrations up to 60 ppm_v. As mentioned previously, H_2S can also be removed from fugitive landfill gas. Two examples of treatment methods are the use of alternative covers and the use of masking agents. Alternative covers are used as a

substitute for conventional cover soil to minimize H_2S emissions by providing a barrier between ambient air and the underlying waste. Various materials have been used, including concrete, sandy soil, and compost (Xu et al. 2010; Yang et al. 2006). The use of masking agents is also common practice for handling odors caused by H_2S. Investigations of such treatments have shown that they can provide temporary relief from odors, but should not be used as a permanent treatment measure (Bruchet et al. 2009).

2.4. Summary

This chapter presented a discussion of topics relevant to the treatment of odors caused by H_2S and the principles utilized to construct and operate the pilot odor control device. Specifically, research about the generation of H_2S in landfills, the factors that influence this generation, and the various technologies used to treat gaseous H_2S were introduced. These topics will serve as the background for the information in the following chapters.

CHAPTER 3: THERMAL REGENERATION OF ACTIVATED CARBON

3.1. Introduction

Granular activated carbon (GAC) is a widely used adsorptive agent for the removal of hydrogen sulfide (H_2S). Its high porosity and extensive surface area make it an extremely effective adsorbent (Benjamin and Lawler 2013). It is one of the best alternatives based on cost and simplicity (Coppola and Papurello 2019). GAC is produced from a variety of carbon sources including coal (Bagreev et al. 2004), wood (Bagreev et al. 2000a), peanut shell (Wang et al. 2020), and coconut shell (Bagreev et al. 2000b), each with varying pore structures and carbon content. GAC is a particularly attractive alternative because of its ability to remove H_2S at low concentrations (Bagreev et al. 2005).

The process of adsorption can be influenced by the physicochemical and structural characteristics of GACs. For example, GAC can be impregnated with cations distributed on the pores of the carbon surface (Henning and Schäfer 1993). NaOH, Na_2CO_3, KOH, KI, K_2CO_3, $Cu(NO_3)_2$, and $FeCl_3$ are examples of compounds used in impregnated GACs (IACs) (Chiang et al. 2000; Huang et al. 2006; Nakamura et al. 1996). The presence of cations in IACs increases the effects of chemisorption, but reduces the amount of physisorption because of the increased number of occupied adsorption sites on the carbon surface (Balsamo et al. 2016; Yan et al. 2004). Adsorption of H_2S can also be influenced by other surface properties of the carbon including pH, pore size distribution, moisture content, and specific surface area (Adib et al. 1999; Bandosz 1999; Huang et al. 2006).

Exhausted GAC can be regenerated instead of discarding or incinerating it. Regeneration can help protect the environment and conserve resources by reducing creation of waste materials. Many methods for regeneration are being investigated, including microwave regeneration, solvent extraction, extraction with supercritical fluids, electrochemical regeneration, and catalytic oxidation (Zhou et al. 2021). Furthermore, the most well-developed method for the regeneration of H_2S-saturated GAC is conventional thermal regeneration. This process has been performed with streams of air and water (Bandosz 2002). Regeneration of H_2S-saturated carbon using water is marginally successful because of the presence of bulky sulfur polymers that are formed on the carbon surface during adsorption (Bagreev et al. 2002). Large sulfur-containing compounds like sulfuric acid are the result of chemisorption that creates a low-pH environment that is difficult to regenerate with water. However, another study successfully removed phenols, textile dyes, and pesticides using liquid water at subcritical conditions (Salvador and Jiménez 1996). Water heated to a temperature of 300°C and pressurized to 120 atm fully regenerated samples of exhausted carbon. Even after five adsorption-regeneration (A-R) cycles, the adsorption of capacity was fully maintained. Thus, higher temperatures and pressures may be necessary for successful liquid-water desorption of H_2S.

Studies have also investigated the use of streams of inert gases for H_2S desorption. The application of thermal treatment by passing inert gases at 300°C over exhausted carbon resulted in significant removal of sulfur species from the carbon surface (Bagreev et al. 2001). When compared with air however, it was determined that the use of nitrogen gas was much less efficient. The amount of sulfur removed from exhausted

samples of carbon was six times greater in samples that were treated with air as opposed to nitrogen. It was postulated that the oxidation of elemental sulfur as well as the reduction of sulfuric acid occurred more readily in an oxygenated air stream. Similar A-R experiments have been completed with phenol-based compounds using microwave heating technologies (Ania et al. 2004). Experiments done at 1,123 K showed that thermal regeneration was favorable under a CO_2 atmosphere compared to an inert atmosphere (N_2). This further confirms the theory that an oxidizing atmosphere is essential for effective regeneration.

In this chapter, an explanation of a series of performed A-R experiments will be provided. Regeneration of spent GAC was carried out in columns under various temperatures. The GAC was saturated with H_2S and adsorptive capacities after successive regeneration cycles were evaluated from concentration data.

3.2. Materials and Methods

Samples of a commercial granular GAC, GC Sulfursorb Plus (General Carbon, USA), were obtained for this study. This GAC was non-impregnated, bituminous coal-based, and developed commercially for the removal of H_2S from air streams. It has an approximate particle diameter of 3.4 mm.

The carbon was packed, as received, into a stainless-steel column (1 in. i.d., 12 in. length). A layer of glass wool and pea gravel was used to secure the carbon inside the column during experimentation.

H_2S was generated by purging N_2 gas through a container containing sodium sulfide with acetic acid. The flow rate of N_2 gas entering the column was maintained at

2.5 L/min. The concentration of H_2S was measured using H_2S gas loggers at the inlet and outlet. The experimental setup is depicted in Figure 3.1.

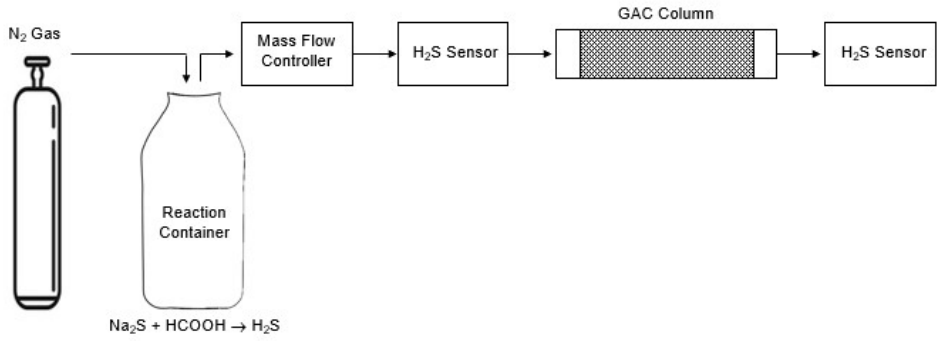

Figure 3.1: Adsorption Experimental Setup

3.2.1. Adsorption and Regeneration Experiments

A series of adsorption experiments were conducted on samples of GAC. During each experiment, the GAC was subjected to a constant stream of gas containing a measured, but constantly changing concentration of H_2S. Data was recorded continuously at 10-second intervals with the use of H_2S sensors placed at the inlet and outlet of each column. The test ended when the influent concentration reached zero following the beginning of the H_2S-producing reaction. Each adsorption experiment was carried out at room temperature (approximately 25°C). The adsorption capacity and efficiency was calculated using the weight of the carbon, flow rate, and the H_2S concentration in the inlet gas and outlet gas. During thermal regeneration, the column containing the GAC sample from the adsorption experiment was heated using heat tape to the designated temperature of 500°C. During heating, the ends of the column were sealed to prevent any

H_2S from escaping the column volume. Upon reaching the temperature set point, a stream of nitrogen gas was passed through the saturated column at a flow rate of 2.5 L/min. Concentration measurements were taken from the outlet of the column with the previously mentioned gas data loggers until the concentration of H_2S leaving the column was negligible. The regeneration efficiency for each sample of carbon was calculated for each successive adsorption run following regeneration. This series of experiments was conducted on three samples of carbon for three cycles each.

It should be noted that the placement of the mass flow controller downstream of the reaction vessel is not advised for future experiments. Repeated exposure to H_2S, especially in higher concentrations, can corrode the sensitive components of the controller which would cause the calibration to drift. It is recommended to instead place the mass flow controller upstream of the reaction vessel to prevent interactions between manufactured H_2S and the controller.

3.2.2. Material Characterization

Various physical characteristics of the GAC were explored to understand the results of the experiments better. Several tests were conducted to quantify these characteristics which, include elemental composition, specific surface area, micropore volume, and pore size distribution. Four samples were investigated: a fresh (virgin) carbon sample (Carbon I), a carbon sample that had reached breakthrough (Carbon II), a carbon sample that had been thermally regenerated (Carbon III), and a carbon sample that had reached breakthrough following regeneration (Carbon IV). The surface morphology and the elemental content of these samples was measured with a scanning electron microscope (SEM) and energy dispersive X-ray analysis (EDX). SEM and EDX

measurements were performed using an FEI Nova NanoSEM 450 (University of Nebraska-Lincoln). The carbon was also characterized with nitrogen sorption isotherms at a temperature of 77 K using a computer-controlled Micromeritics ASAP 2460 apparatus (Micromeritics Instrument Co., Norcross, GA, USA). These isotherms were used to determine the specific surface area by applying the Brunauer, Emmett and Teller (BET) method. The calculation of the micropore volume (pores < 2 nm) was accomplished using the t-plot method.

3.3. Results and Discussion

3.3.1. Adsorption

In many of the experiments, the GAC samples experienced breakthrough shortly after the beginning of the H_2S-producing reaction. A plot of consecutive breakthrough curves for one of the GAC samples is shown below in Figure 3.2. The first cycle showed an excellent capture of H_2S, with minimal breakthrough. The amount of H_2S captured by the GAC decreased in subsequent cycles, indicating that the capacity of the GAC to adsorb H_2S decreased after the first regeneration. For the sake of simplicity and to reduce the effect of experimental error, the adsorption capacity of the GAC used in these experiments was estimated based on its performance in a virgin cycle where breakthrough was negligible. The amount of H_2S that was adsorbed in the first cycle shown below is approximately 2.0 mg. This value, which corresponds to an adsorption capacity of 0.4 mg/g, was used as a baseline to later calculate the efficacy of thermal regeneration. This adsorption capacity closely resembles values found in similar studies. One study reported an H_2S adsorption capacity of 0.5 mg/g for an NaOH-impregnated GAC (Sitthikhankaew et al. 2011).

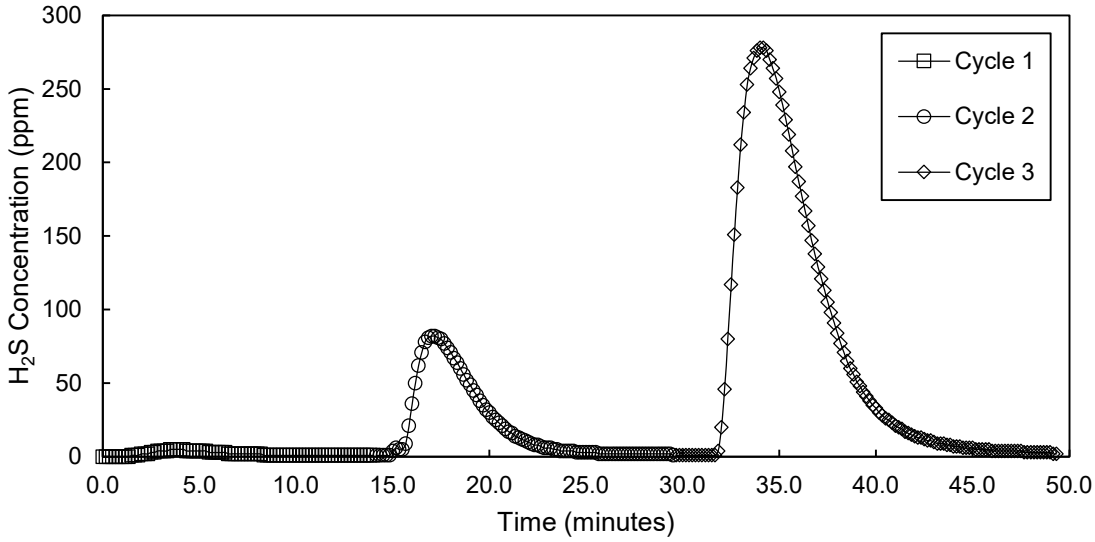

Figure 3.2: Successive Adsorption Cycles

Over the course of experiments with three samples of GAC which included three consecutive cycles with three different samples, the average adsorption efficiency was approximately 82%. The average effectiveness for each cycle was 94%, 74%, and 79% for the first, second, and third cycles, respectively. This data suggests that the carbon used in these experiments has a good adsorption efficiency in its virgin state but drops considerably after its first regeneration. Nonetheless, the adsorption capacity seemed relatively constant in the second and third cycles.

3.3.2. Thermal Regeneration

After each sample of GAC was subjected to a stream of H_2S, the carbon was regenerated by heating to a temperature of 500°C. Curves showing the concentration of H_2S during successive regenerations for the same sample as in Figure 3.2. appear in

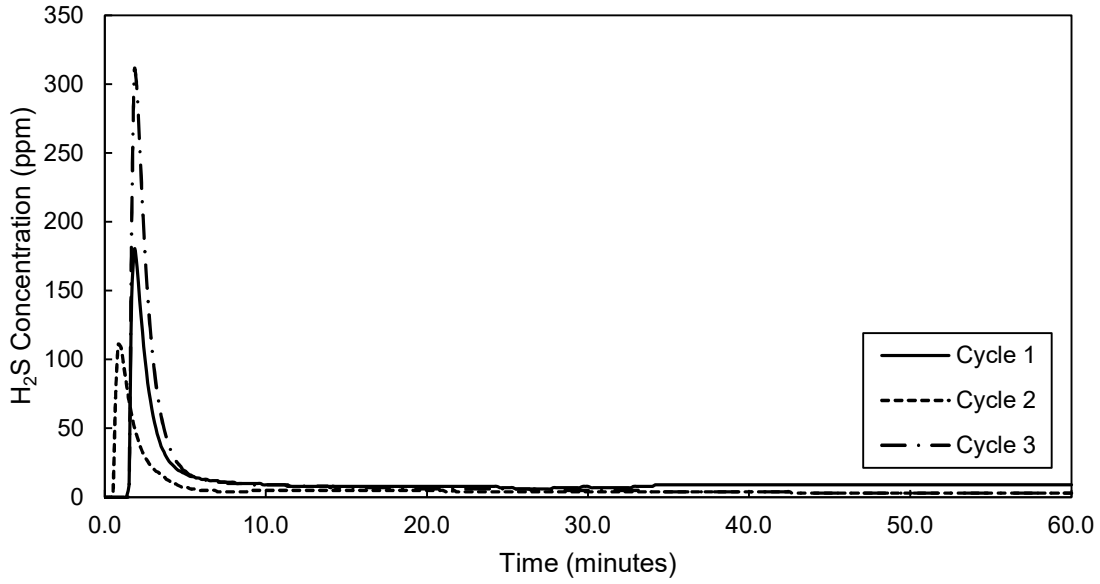

Figure 3.3: Successive Desorption Cycles

Figure 3.3. The height of each peak in Figure 3.3 varies based on the magnitude of H_2S that was introduced to the carbon during adsorption. For instance, the calculated amount of H_2S that entered the column was 2.0 mg, 2.2 mg, and 3.5 mg for the first, second, and third cycles respectively. Cycle 1 produced a larger peak than cycle 2 during desorption because a larger amount of H_2S was captured during adsorption. Cycle 3 produced the largest concentration of H_2S during thermal regeneration both because the carbon had been saturated three times and because the input during adsorption was the largest of the three cycles. Therefore, a larger H_2S input provides a higher concentration of H_2S during thermal regeneration. The total amount of H_2S desorbed during the previously described cycles was 1.5 mg, 0.8 mg, and 1.3 mg, respectively. A rough correlation exists between

the amount of H_2S desorbed and the peak concentration in each thermal regeneration experiment. The highest amount of H_2S was desorbed in cycle #1 despite having a lower peak value. This may be due to the large amount of H_2S that was adsorbed in the first cycle and because it was the first thermal treatment. The amount of desorbed H_2S drops in cycle #2 and then increases again in cycle #3, similar to the peak concentrations.

The efficiency of thermal regeneration, like the adsorption efficiencies, were good during the first cycle, but declined in subsequent cycles. The efficiencies for each sample and its three cycles are shown below in Table 3.1.

Table 3.1: Calculated Regeneration Efficiencies

Sample	Cycle 1	Cycle 2	Cycle 3
Sample 1	52%	15%	57%
Sample 2	79%	40%	69%
Sample 3	78%	55%	31%
Average:	**70% ± 12%**	**37% ± 12%**	**52% ± 12%**

The average regeneration efficiency for the cycle completed with virgin samples of carbon was approximately 70%. The efficiencies for the second and third cycle were 37% and 52%, respectively. The regeneration efficiency for Cycle 2 is noticeably lower than the others due to the first sample's efficiency of 15%. A possible explanation for this may be that the sample of carbon did not receive sufficient heat to remove the adsorbed H_2S. If this outlier is removed from the data set, the average efficiency for the second cycle rises to about 47%. This value is much nearer to the efficiency of the third cycle. Overall, these results suggest that the regeneration efficiency is greatest during the first cycle, drops in subsequent cycles, but remains constant thereafter. This is an

indication that several of the pores in the GAC become permanently occupied after one round of adsorption . Thermal regeneration may be inadequate for removing some of the H_2S after the first cycle.

3.3.3. Activated Carbon Characterization

The specific surface area of the samples is a primary indicator of their ability to adsorb contaminants. A summary of the characteristics of the four samples is presented in Table 3.2. The BET surface area of the carbon samples ranged from 372 m^2/g to 441 m^2/g. This is lower than typical values for granular GACs, but not unlike some carbons developed from coconut shell, which can have BET surface areas around 380 m^2/g (Singh et al. 2008). Each value was calculated from its respective nitrogen sorption isotherm. Carbon IV demonstrated the highest value of specific surface area as well as the highest total pore volume. This indicates that it may have the highest physical adsorptive capacity of the four samples. In contrast, Carbon II showed the lowest surface area and total pore volume, which both sharply declined compared to Carbon I. This was most likely a result of the deformation that occurred after thermal regeneration.

The isotherms of Carbon I-IV are shown below in Figure 3.4. All the carbon samples displayed IUPAC type-I isotherms. Each of the carbons demonstrates a significant increase in nitrogen adsorption at higher relative pressures, evident by the "ski-jump" shape in each isotherm. The hysteresis loops in each isotherm are well-pronounced, which suggests that each of the carbon samples have a well-developed

Table 3.2: BET Surface Area and Micropore Volume for Carbons I-IV

Sample	BET Surface Area (m^2/g)	t-plot micropore volume (cm^3/g)	Total Pore Volume (cm^3/g)	Average Pore Diameter (nm)
Carbon I	433	0.126	0.311	3.341
Carbon II	372	0.103	0.268	3.343
Carbon III	397	0.096	0.342	3.623
Carbon IV	441	0.112	0.356	3.514

microporosity and mesoporosity. The four samples of GAC were analyzed using SEM/EDX and the results of the elemental analysis appear in Table 3.3. The accompanying spectra also appear in Figure 3.5. SEM photographs of each of the samples (5000X magnification) in Figure 3.6. show the porous structure of each sample, including some mesopores with distinct shapes and roughness. Micropores were visualized at higher magnifications, which appear in Appendix C.

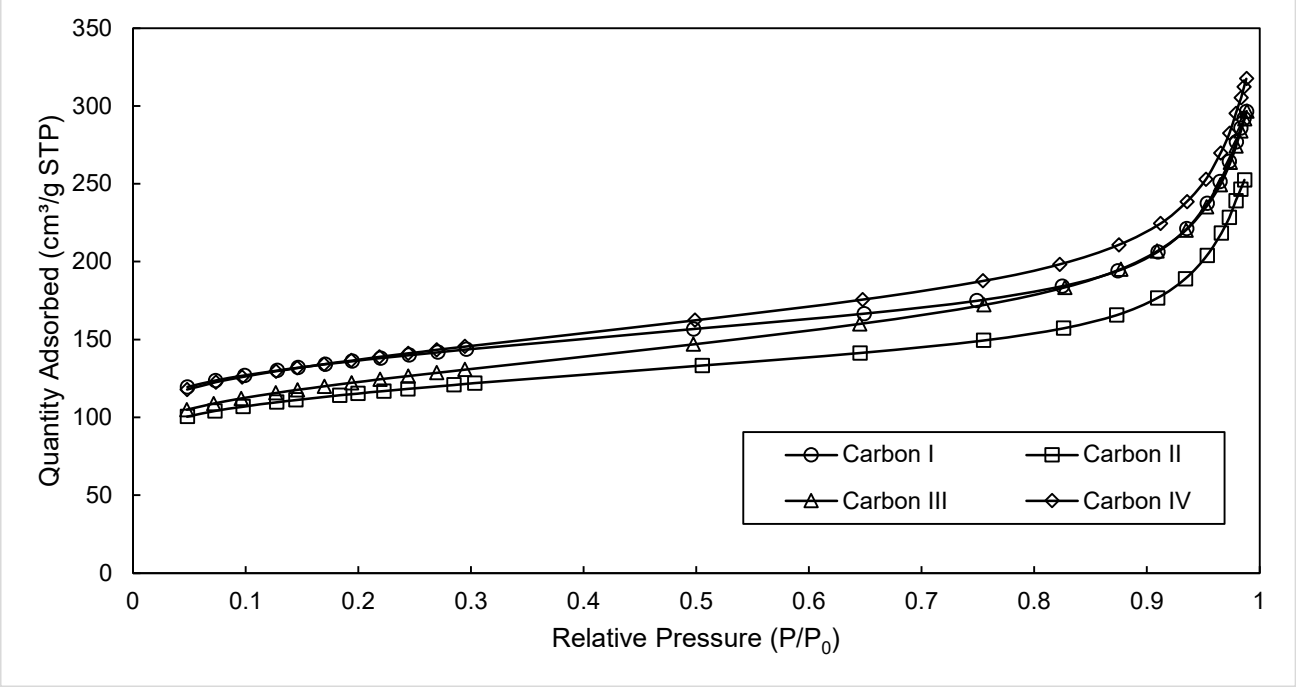

Figure 3.4: Adsorption/Desorption Isotherms for Carbons I-IV

According to the analysis presented in Table 3.3, the sulfur content of the samples increased after each adsorption cycle, as expected. The weight fraction of sulfur doubled during the first run but increased by only approximately 30% during the second cycle. The amount of sulfur also notably decreased after thermal regeneration from 2.6% to 2.2%. This is an indication that some of the adsorbed sulfur was effectively removed through thermal regeneration, but not all of it. This finding agrees with the results obtained from the cyclic experiments. Furthermore, it is known that thermal regeneration with the use of nitrogen does not remove sulfur-containing compounds from GAC as well as oxygenated air (Bagreev et al. 2001). This is because elemental sulfur cannot be oxidized in the presence of nitrogen gas.

The amount of oxygen fluctuates for each sample but stays relatively constant. During the adsorption experiments described previously, a nitrogen stream was used to transport H_2S to the carbon. It may be possible that some of this nitrogen stream became adsorbed to the surface of the carbon and this mass of nitrogen replaced the weight of oxygen, thus resulting in a loss of oxygen during each period of adsorption. In many instances, unless there is an unusually high amount of nitrogen on the surface of the carbon, the carbon peak will conceal the nitrogen peak. Therefore, the nitrogen peak does not appear in Figure 3.5.

Table 3.3: EDX Analysis for Carbons I-IV

EDX Analysis for Carbon Samples (Wt. %)				
Element	**Carbon I**	**Carbon II**	**Carbon III**	**Carbon IV**
C	65.1	73.3	64.5	69.2
O	11.4	10.1	14.4	13.3
Na	0.4	0.0	0.0	0.0
Mg	1.3	0.7	1.5	1.2
Al	2.0	1.1	1.4	0.7
Si	2.3	1.7	1.6	0.4
S	1.3	2.6	2.2	2.9
Ca	12.9	8.1	10.2	7.6
Fe	3.5	2.3	4.3	4.6
Total	**100**	**100**	**100**	**100**

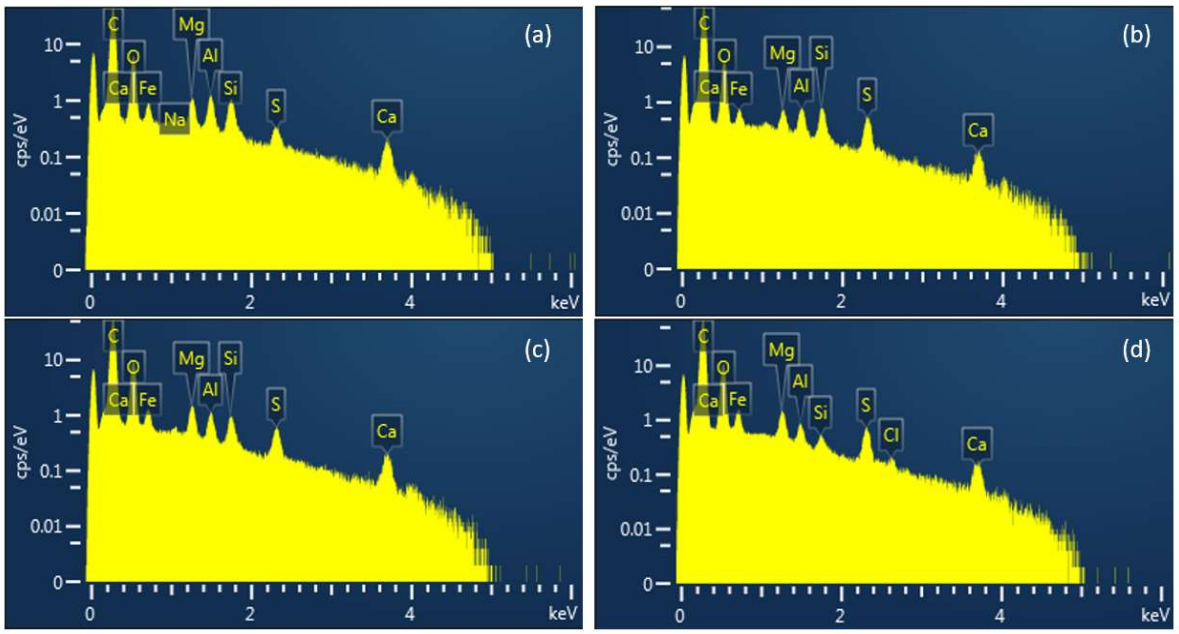

Figure 3.5: EDX Spectra for Carbons (a) I, (b) II, (c) III, (d) IV

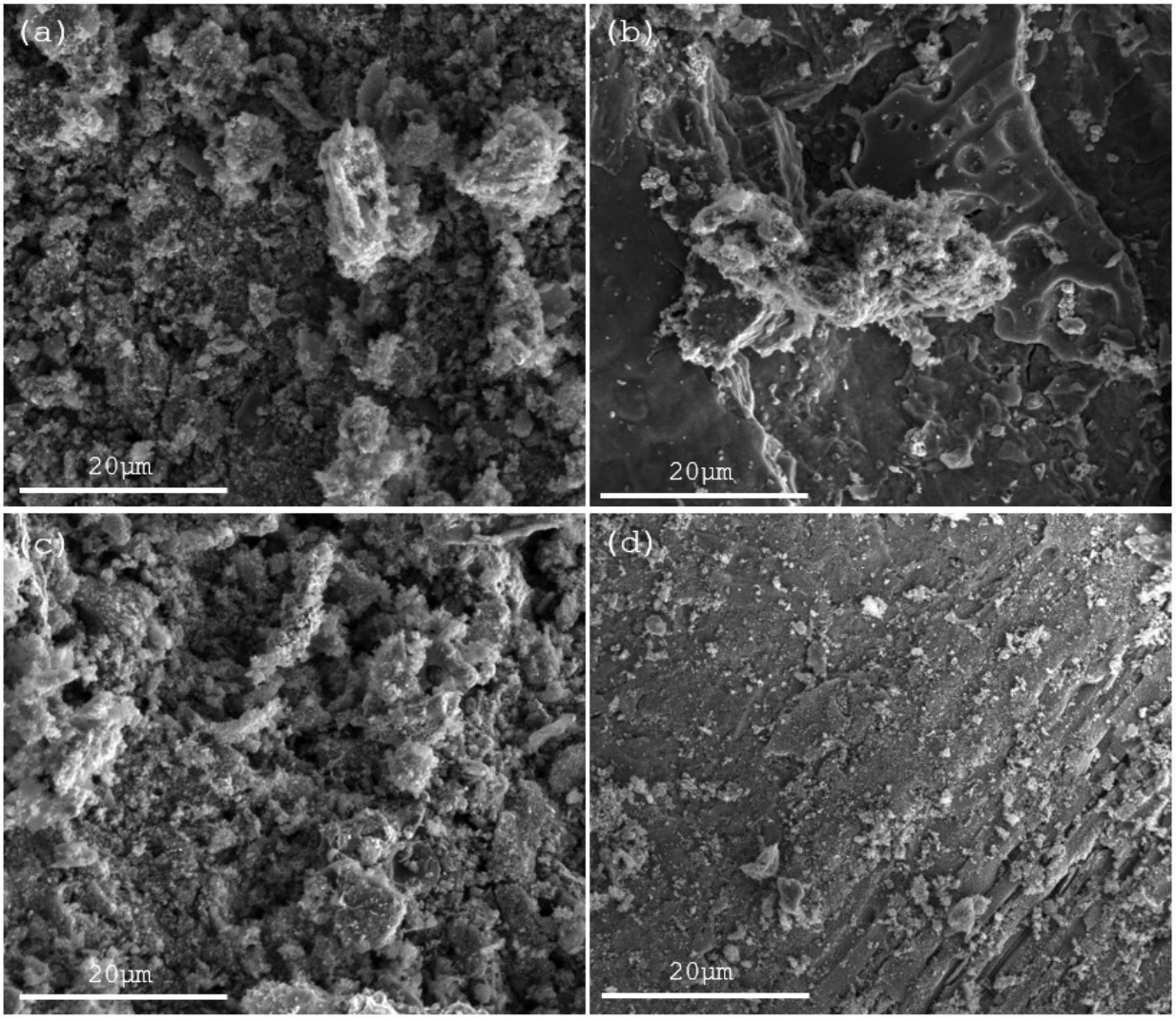

Figure 3.6: SEM Images for Carbons (a) I, (b) II, (c) III, (d) IV

3.4. Conclusion

The primary objective of the experiments described in this chapter was to investigate the concept of thermal regeneration of GAC. Though the regeneration efficiencies are not as high as other studies have reported, successful regeneration of saturated carbon was observed. The application of this concept is foundational to the operation of the pilot odor control device which will be discussed in subsequent chapters.

Results from the experiments indicated that after being saturated with H_2S, GAC can be effectively regenerated at high temperatures. The samples used in these experiments were regenerated at an efficiency of approximately 70% after one adsorption cycle with lower efficiencies in later cycles, A temperature of 500°C is suggested to remove the sulfur-containing compounds from the GAC. The application of this amount of heat within the pilot device and its effectiveness in the field will be further explored.

CHAPTER 4: TEST SITE DESCRIPTION AND ANALYSIS

4.1. Introduction

The Loup Central Landfill is a relatively small landfill located in central Nebraska. This site was selected for the placement of the pilot device to improve air quality for the public. The site selection was based, in part, on the requirements of the grant that funded the project by reducing odors caused by H_2S. The Loup Central Landfill is in one of the counties that receives the lowest funding from the Nebraska Environmental Trust (NET). Additionally, once transported to the landfill, the pilot device could be placed in a location that does not interfere with daily operations. These factors, along with the full collaboration of the landfill operator, provided sufficient cause to select the Loup Central Landfill as the operating site for the pilot device.

The pilot device is a three-part apparatus that captures, concentrates, and treats gas containing odorous compounds. To demonstrate the effectiveness of these functions, the pilot device needed to be tested at a site with off-gas that contained a reasonable concentration of H_2S. Therefore, prior to the construction of the pilot device, gas emitted from the leachate collection system at the Loup Central Landfill was analyzed at several locations to determine its viability. The tests included analysis of the compounds found in the off-gas, properties of the leachate produced by the landfill, and an analysis of the leachate cleanout system. Samples of off-gas were collected from cleanout wells around the landfill, each numbered in red in Figure 4.1. An investigation of the leachate cleanout system and the H_2S concentrations of the off-gas samples were used to determine the optimum location to place the pilot apparatus.

4.2. Description of the Loup Central Landfill

The Loup Central Landfill is located three miles south of Elba, Nebraska and is owned and operated by five counties: Howard, Sherman, Greeley, Loup, and Garfield. It has been in operation since 1996 and consists of four different physical sections: Phase 1, Phase 2, Phase 3, and Construction & Demolition section. Each section of the landfill is visible in Figure 4.1. The red numbering indicates the location of leachate collection wells.

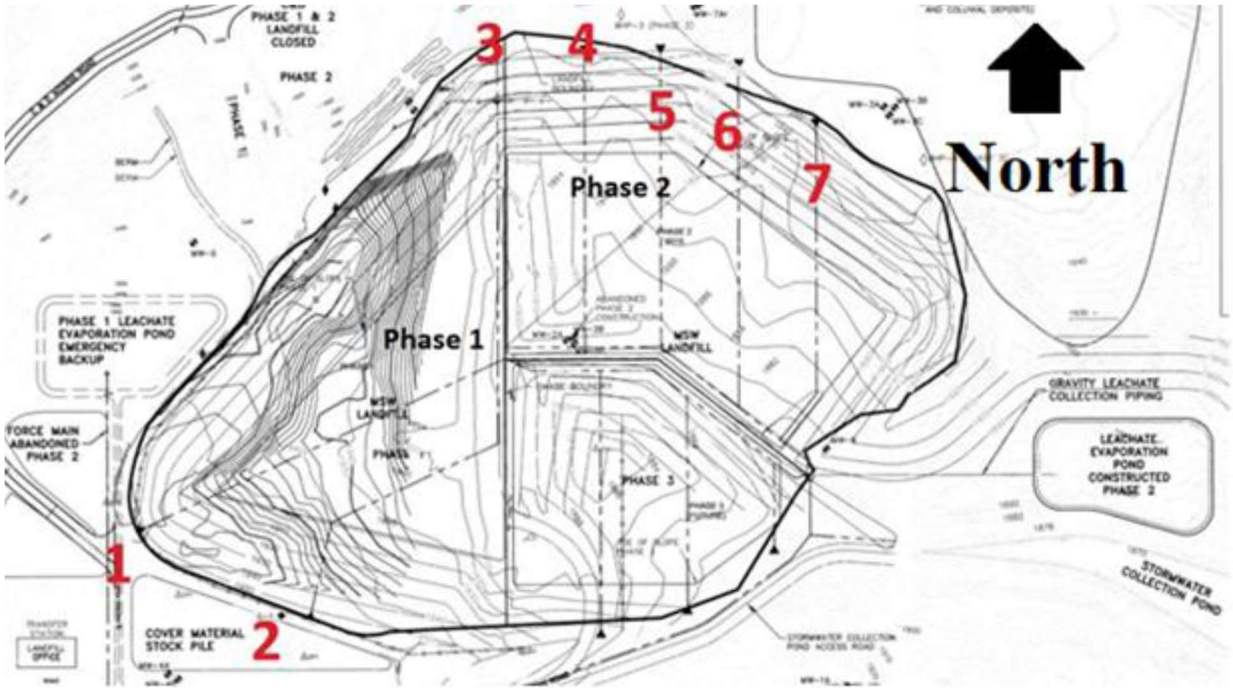

Figure 4.1: Leachate Cleanout Locations

Phase 1, which consists of 7.5 acres, was the first area to be used for the containment of solid waste. Between 1996 and 2016, it was filled with an estimated 402,000 square yards of household waste (Cohen 2020). The depth of the waste is approximately 50 feet. In 2016, Phase 1 had an intermediate soil cover placed over the top of the waste to a depth of two feet. It has been inactive ever since (Cohen 2020). Phase 2 is currently being used for household wastes. It has an area of 10 acres and an estimated capacity of 412,000 square yards. Additionally, it has a life expectancy of twelve years. Phase 3 will begin receiving household waste disposals once Phase 2 has reached its full capacity. It has an expected lifespan of 18 years and a capacity of 621,000 square yards (Olsson, 1996). The construction & demolition cell, which contains waste generated from construction projects, is located the north side of the landfill.

The leachate cleanout system is a network of solid and perforated piping that is located under Phases 1 and 2. The piping collects liquid leachate from the bottom of the landfill and feeds to a collection pond. The piping is connected to a total of seven cleanout wells at the boundaries of Phase 1 and 2. The vapor in these wells rises to the surface, where it can be captured and analyzed.

4.3 Gas Collection and Analysis

The off-gas generated by the Loup Central Landfill was collected from the leachate cleanout system on multiple dates and times and tested for H_2S concentration, temperature, flow rate, and chemical composition. Sampling was completed throughout 2020 to obtain data based on a range of conditions that would be supplied to the pilot device (Cohen 2020). This data helped determine the design constraints for the pilot apparatus. Many landfills have gas collection systems which can provide a simpler

means for treating landfill gas emissions, and often provide higher concentrations of H_2S (Omar and Rohani 2015). However, as the Loup Central Landfill does not possess a gas collection system, the leachate cleanout system was selected as the source for gas treatment.

An air pump with flexible tubing was used to collect samples that were analyzed using Jerome H_2S units. This data served as the primary basis for the determination of the cleanout well that would serve as the source of off-gas for the pilot device.

The concentration of H_2S in three cleanout wells was recorded and analyzed. Cleanout well #3 (see Figure 4.1) did not provide a level of H_2S that would be sufficient for operating the pilot device. Furthermore, that well was located far away from the landfill office building and would be more difficult to reach with utilities. Cleanout wells #1 and #2 showed a promising concentration of H_2S during sampling (see Figures 4.2 and 4.3). Both cleanouts produced gas with an H_2S concentration of approximately 40 ppm.

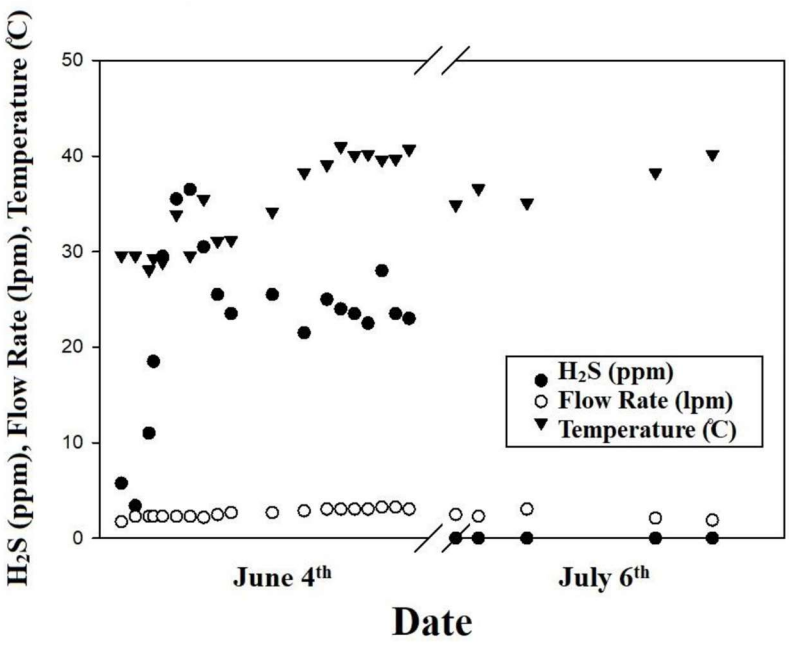

Figure 4.2: Off-Gas Data from Cleanout #1 (from Cohen 2020).

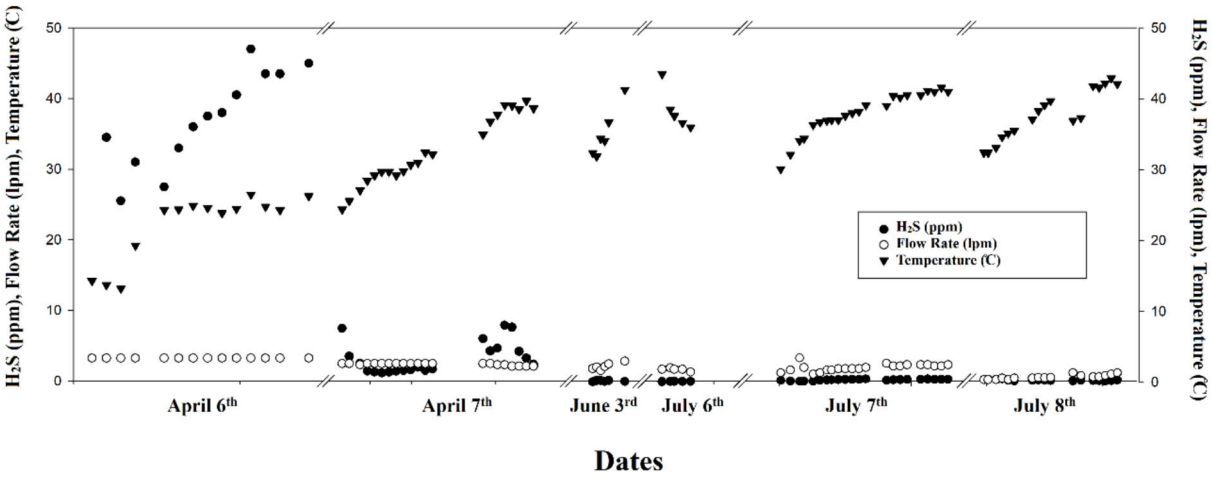

Figure 4.3: Off-Gas Data from Cleanout #2 (from Cohen 2020).

During subsequent sampling periods, however, the concentration of H_2S seemed depleted. This indicates that the concentration of H_2S in the cleanout is volatile and may be affected by sampling. Nevertheless, Cleanout #1 was chosen as the site for operation of the pilot device because of its proximity to the operations building. Micro-GC analysis (Agilent 2022) was also conducted on samples of the off-gas collected from the cleanouts at the Loup Central Landfill. Three grab samples, each with three replicates, were analyzed. The results of this analysis identified a possible explosion risk as one sample of CH_4 and all three samples of H_2 showed concentrations that were within their respective upper and lower explosive limits. The concentration of CH_4 in question was 14% and the concentrations of H_2 ranged from 13 – 29% (Cohen 2020). Typical landfill gas consists of roughly 50% CH_4 and 50% CO_2, thus these values are unusual (Omar and Rohani 2015) . It should be noted that these limits differ from values at atmospheric conditions based on the concentration of O_2 and CO_2 in the landfill gas (Liu et al. 2018). Regarding this point, analysis showed O_2 concentrations well above 100% which is an indication of

possible experimental error. Nonetheless, caution is recommended and methods for mitigating the risk of autoignition will be discussed in Chapter 5.

4.4. Summary

The primary objectives of this chapter were to provide a thorough description of the chosen site for the pilot odor control device and to briefly summarize the analyses that were conducted to investigate the characteristics of the off-gas within the leachate collection system. This information servers as the basis for the construction of the pilot odor control device which is discussed in the following chapter.

CHAPTER 5: CONSTRUCTION AND OPERATION OF PILOT DEVICE

5.1. Introduction

A pilot odor control device with the ability to capture, concentrate, and treat odors in landfill gas was constructed for operation at a small, remote landfill site. The analyses described in Chapter 4 laid the groundwork for the installation of this device and its operation. Construction of the device was guided by a proposed design which was modified slightly to accommodate its use at the testing site. During the operation of this device, data was collected to accomplish three primary goals to validate the device's effectiveness. The objectives were to analyze (I) the gas entering the treatment system, (II) the concentration of the gas as it moves through the system, and (III) the treatment efficiency of the BTF.

5.2. Design Summary

The operation of the pilot device can be divided into four main components: (i)

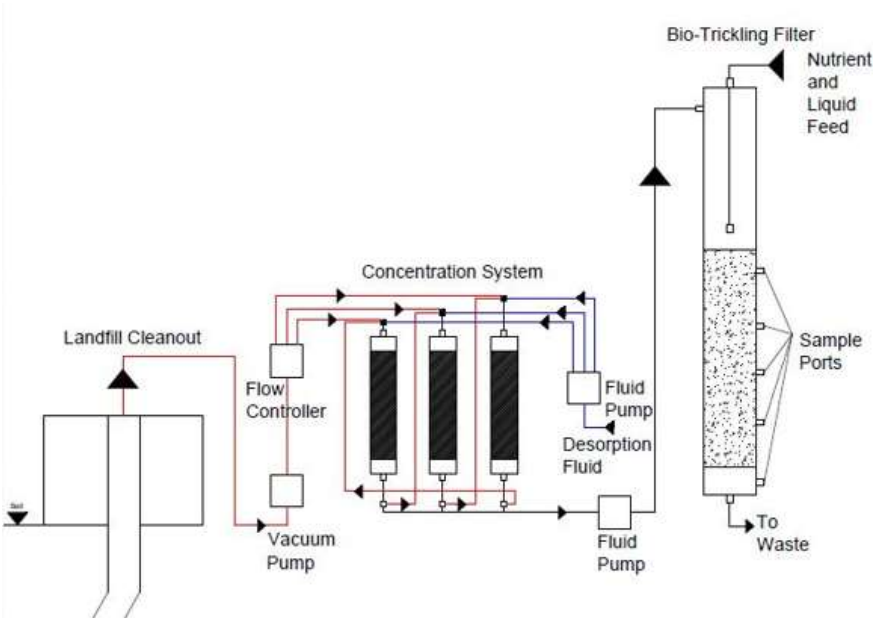

Figure 5.1: Proposed Design (from Cohen, 2020)

capture, (ii) concentration, (iii) transport, and (iv) treatment. The initially proposed system, shown in Figure 5.1, depicts a system that (i) captures the gas via a vacuum pump, (ii) concentrates the gas with three GAC columns, (iii) transports the gas via flexible tubing and solenoid valves, and (iv) treats the gas with a BTF. This design was used for the construction of the pilot odor control device with various modifications that will be discussed throughout this chapter. Each component of the device will be described subsequently.

5.2.1. Gas Capture System

The portion of the odor control device responsible for extracting the landfill gas and sending it for treatment is comprised of a regenerative blower and PVC fittings that provide a seal on the cleanout well opening, as illustrated in Figure 5.2 and Appendix A. The regenerative blower was selected based on various process requirements. Specifically, a regenerative blower with an explosion-proof motor was selected to

Figure 5.2: Gas Capture System

mitigate the risk of autoignition discussed in Chapter 4. It is important to note that using conduit to contain the electrical wiring would be necessary to fully prevent the risk of explosion. The setup pictured above does not safely prevent the interactions between the motor and the surrounding air.

A consideration of the needed discharge and head throughout the system was also necessary. Pressure testing with available pumps on the piping informed the selection of the blower. The flow rate was then adjusted with a gate valve to meet the residence time requirements of the BTF.

5.2.2. GAC Concentrator System

Two GAC columns comprise the concentrator system which is designed to saturate a bed filled with GAC with H_2S, desorb the H_2S via thermal regeneration, and allow the concentrated gas to move to the BTF for treatment. Two columns are used instead of three as proposed in the original design to simplify the flow scheme and to reduce pumping requirements. The carbon columns are connected in series with the gas extraction system and are suited to withstand the amount of heat needed to desorb H_2S from the GAC. The columns are packed with GAC, mounted on steel framing, and wrapped in high-temperature insulation to reduce the amount of heat transfer laterally down the piping, clearly visible in Figure 5.3. Additionally, they are connected to the system with stainless steel fittings, which provide a thermal buffer for the PVC piping used in other parts of the system. The columns are heated by small lengths of heat tape connected to a PID controller. They are both pictured along with the air compressor that provides purging air during desorption.

The GAC columns are set up in parallel but do not run simultaneously. The columns receive gas from the landfill for an extended period to collect a large amount of lower concentration H_2S. Then, during heating, a relatively smaller amount of higher concentration H_2S is removed from the column during the application of heat and purging air. The columns are designed to retain heat up to 500°C based on experiments described in Chapter 3.

Figure 5.3: GAC Concentrator System

5.2.3. Gas Transport

The air moving through the pilot odor control device is transported by a network of pipes and valves. Four solenoid valves are used to direct the flow of air to either of the two GAC columns. These solenoid valves are operated via an irrigation controller which turns the solenoid valves on at specified times during operation. The irrigation controller itself does not provide enough current to power the solenoid valves; therefore, a transformer that provides an identical voltage is used with a relay to open and close these valves. The two solenoid valves pictured in Figure 5.4 are used to control the air that

enters the GAC columns during thermal regeneration. A diagram that depicts the electrical wiring of this component of this system is shown in Appendix A.

The system also contains swing-type check valves to prevent any backflow. The motivation for these check valves is to keep the flows entering and leaving each GAC column separate. This is especially important as any landfill gas containing a significant amount of methane should remain isolated from a column that is being thermally regenerated to prevent autoignition.

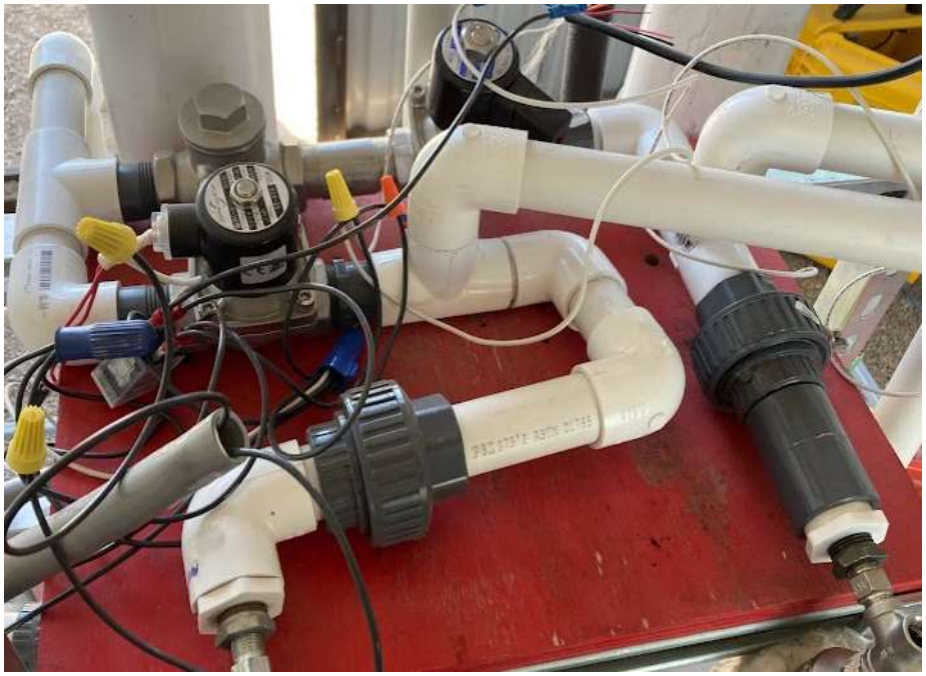

Figure 5.4: Gas Transport System

5.2.4. Biological Treatment

The last stage of the pilot odor control device is biological treatment. The BTF is designed to treat the concentrated H_2S at an effective rate. It is constructed from a PVC pipe containing packing media (MATALA High Density Filter Media) which provides structural support for the microorganisms (see Figure 5.5). To inoculate the BTF, the packing media was seeded with a sample of return activated sludge (RAS) for two days

and then nourished with regular additions of nutrient solutions. During the start-up phase, the microorganisms were also acclimated to operating conditions with regular additions of H_2S. This process would help prepare the bacteria for daily operations at the landfill site.

Two nutrient solutions are used to cultivate the micro-organisms. The first solution is a simple mixture of glucose and water. The second is a mixture of nutrients including nitrogen, phosphate, potash, boron, copper, iron, and zinc. The solutions provided to the BTF are alternated in between water purges to avoid the build-up of bacteria within the tubing that carries the solution.

Gas from the landfill was supplied to the BTF at a rate that allowed for a residence of time of at least 30 seconds. This value is higher than most full-scale BTFs (Gabriel and Deshusses 2003).

Figure 5.5 Biological Treatment

5.3. Testing of Pilot Odor Control Device

A series of tests were conducted to assess the ability of the pilot odor control device to successfully accomplish the project objectives. Specifically, these tests were designed to answer two questions related to operations within the device. First, the ability of the pilot odor control device to concentrate H_2S needed to be confirmed and quantified. To accomplish this end, gas containing H_2S would need to be adsorbed and subsequently removed via thermal regeneration of the GAC. Second, the treatment efficiency of the BTF needed to be documented, both with the gas leaving thermally regenerated GAC, and with gas supplied directly from the landfill. Several visits were

made to the test site to conduct these experiments and to gather data that would demonstrate its operation. This data was compiled and analyzed.

5.3.1. Methods

Experiments designed to confirm the project objectives were performed at the test site. Specifically, tests were run to analyze the (I) the gas entering the treatment system, (II) the concentration of the gas as it moves through the system, and (III) the treatment efficiency of the BTF.

In completing these tests, data was obtained during several visits to the Loup Central Landfill. The visits spanned over roughly three months of time between March and May, which provided a range of testing conditions. Additional experiments were completed after the device was transported back to the University of Nebraska-Lincoln. These experiments took place on June 27 and June 28.

During experimentation at the Loup Central Landfill, there was no H_2S detected in gas emitted from the leachate cleanouts despite regular samples taken during each visit. It is likely that the lack of moisture during the winter months preceding the experiments prevented the production of H_2S in the landfill. Furthermore, the absence of H_2S necessitated the addition of manufactured H_2S to the gas extracted from the leachate cleanout to simulate treatment of landfill gas containing H_2S. This was accomplished by producing a buffered solution with sodium sulfide (NaS) in water to produce the gas, which was introduced to the air stream with a vacuum pump. This procedure was similar to the one described in Chapter 3. The concentration of H_2S added to the system varied as the reaction progressed, which allows for a fuller view of the treatment capability of the pilot odor control device. A visualization of this process is shown in Figure 5.6.

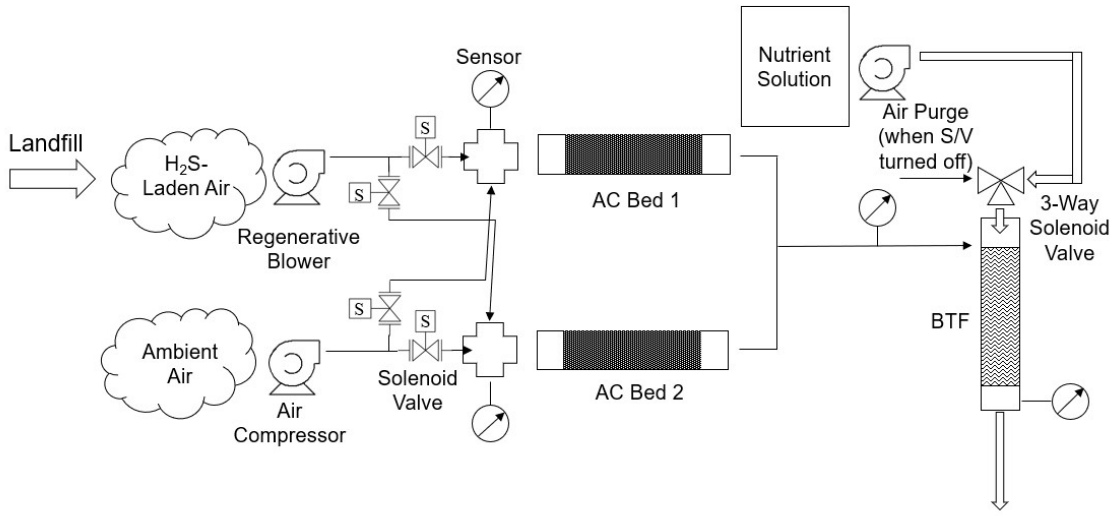

Figure 5.6: Process Schematic of Odor Control Device

Moreover, manufactured gas containing H_2S was monitored during cyclic adsorption-desorption experiments. This gas was pumped into the GAC columns and then subsequently desorbed via thermally regeneration. The GAC columns were packed with roughly 20 grams of GAC (GC Sulfursorb Plus, General Carbon, USA) and supported with a layer of glass wool and pea gravel, like the experiments explained in Chapter 3. A set of ACRULOG H_2S sensors were used to take continuous measurements of the air moving through the GAC columns during testing. The flow rate of the gas entering the GAC columns was approximately 3 cubic feet per minute (CFM). The capture efficiency was calculated using the inlet and outlet concentrations and input and output flow rates. An example of one of these calculations can be found Appendix E.

The sensors were placed inside a low-range sampling system that provided gas samples at a specified volumetric rate of 0.25 L/min, or roughly 0.01 CFM. Connections from this system were made to the inlet of each GAC bed, the inlet of the BTF, and the outlet of the BTF during sampling. These locations are indicated in the process schematic below (Figure 5.6).

The efficiency of the BTF was also investigated. During the thermal regeneration of the GAC columns, measurements were taken at the inlet and outlet of the BTF. The flow rate of gas into the BTF was approximately 1 CFM which corresponded to an empty-bed residence time of 30 seconds. A handful of tests were completed to confirm the presence of bacteria inside the BTF. At various times, the carbonaceous oxygen demand (COD) of the influent nutrient solution was compared with the liquid effluent. Hach TNT 820 (US EPA Reactor Digestion Method: 10211) was used to test the COD of each sample. A dilution of 6:1 was used for the influent solution and a dilution of 3:1 was used for the effluent. A decrease in COD indicated microbial activity.

5.3.2. Results and Discussion

Several experimental runs were completed to test the adsorptive capabilities of the GAC beds. Data was obtained from both the inlet and outlet of GAC columns. An example of one of these runs is shown in Figure 5.7.

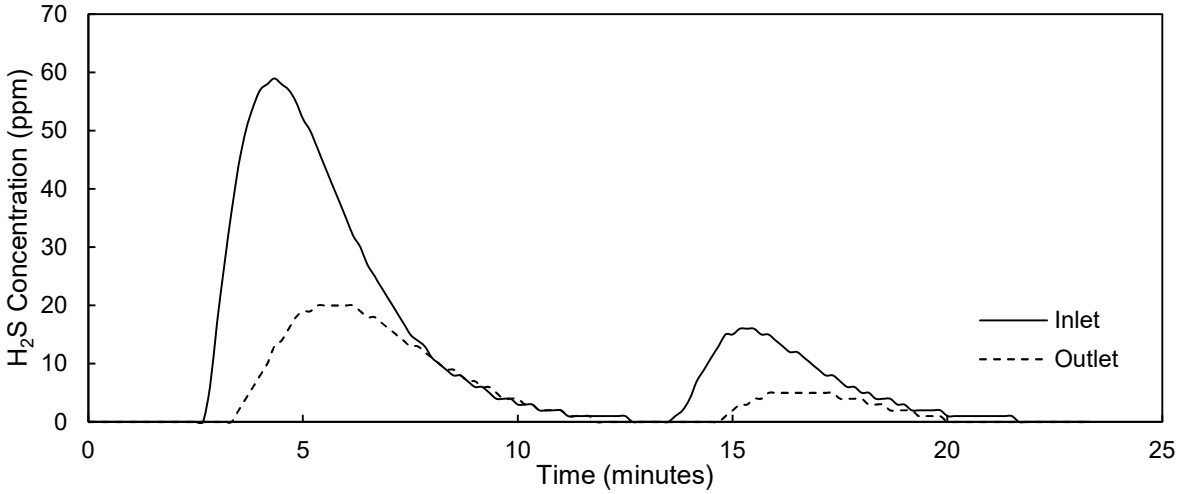

Figure 5.7: Selected Adsorption Curve

Overall, the GAC performed well under experimental conditions. The average capture rate over the course of the experiments was approximately 73 ± 15%. A weighted average of the capture rates based on the average concentration that the bed experienced during a particular run was about 78 ± 15%. A range values between 0 ppm and 50 ppm were introduced to the GAC columns throughout the course of the H_2S reactions. However, the GAC experienced an average concentration of roughly 4 ppm, which is in the same range of concentrations previously documented at the Loup Central Landfill. A summary of data from the adsorption experiments appears in Table 5.1. No trend seems to exist between the cycle number and the capture efficiency, but there appears to be a correlation between the length of the adsorption run and its corresponding capture efficiency. As the length of the run increases, the capture efficiency decreases, which indicates that the adsorptive capability drops as adsorption progresses.

A clear difference exists between the data taken during experiments that took place in May and in June. The capture efficiency seems to be much higher for the data that appears in June. The experiments in June were conducted at a location on the University of Nebraska-Lincoln campus, which means that it was not landfill gas, but ambient air containing H_2S that was introduced to the pilot device. This difference could help explain the difference in capture efficiencies. The lack of competitive adsorption could certainly improve the capture efficiency of the GAC used in these experiments.

Table 5.1: Adsorption Experimental Data

Date	May 13	May 23	May 23	May 23	June 27	June 27	June 28
Cycle Number	1	1	2	3	1	2	3
Length of Adsorption (minutes)	23	36	34	26	15	10	17
Capture Efficiency	60%	53%	66%	64%	96%	85%	87%[1]
Average Concentration Encountered (ppm)	3	4	4	1	4	4	13

The capture efficiency of the activated carbon suffered due to the air velocity of the carbon bed, which was approximately 4 m/s. Such a high air velocity reduces the interactions between gaseous H_2S and the surface of the GAC. A typical design air velocity for GAC used in gas treatment is much lower, typically around 0.5 m/s. Despite this fact, the GAC was relatively effective in capturing H_2S as previously mentioned. The capture of H_2S by GAC was not the primary objective; instead, the goal of H_2S capture was the concentration of the gas. Consideration of the pilot device's ability to concentrate gas requires investigation of data from thermal regeneration experiments.

During thermal regeneration, measurements were taken at the outlet of the GAC columns. Several cycles were completed with each sample of carbon, including a total of 3 hours of operating time. Maintaining the GAC at the suggested temperature of 500°C proved to be a challenge. Upon reaching this temperature, an exothermic reaction would take place, which would cause rapid heating to occur and a dramatic increase in temperature. This observed event was presumably an exothermic reaction caused by

[1] Based on data obtained from a sensor that was out of range for a brief time during experiment.

ignition of the GAC. This reaction was not observed in previous experiments described in Chapter 3 as the gas used during thermal regeneration was inert (without oxygen).

Along with a sharp increase in temperature, the H_2S sensors also detected an overwhelming amount of H_2S in the air exiting the heated columns. This amount of H_2S was far greater than the amount introduced to the columns during adsorption. Consequently, the sensors used in these experiments have a significant cross interference with sulfur dioxide (SO_2); 1 ppm of SO_2 causes an interference of up to 1 ppm. It is known that H_2S, during thermal regeneration, is oxidized to SO_2 and H_2SO_4, among other intermediate species. Furthermore, an experiment was conducted by heating a virgin sample of GAC to 500°C in order to determine if the carbon itself was producing a detectable amount of H2S/SO2. A large amount of H2S/SO2 was detected which is an indication that SO_2 produced by the heated carbon was identified by the sensors and produced inaccurate results. For this reason, the columns were heated to temperatures lower than 500°C with the goal of regenerating the carbon as efficiently as possible without causing ignition.

The results of the thermal regeneration showed that the carbon was regenerated at an overall efficiency of 76 ± 28%. On the experiment conducted on June 28, there was a noticeably lower recovery of H_2S. It is unclear what caused this low result, but it is possible that either the heating was ineffective in removing H_2S from the GAC after the previous two adsorption cycles, or that there was some experimental error. Overall, these results compare favorably with the results that were obtained in earlier experiments described in Chapter 3.

It should be noted that the regeneration data from experiments completed on May 23 demonstrated recoveries higher than 100%. This may have occurred because of several factors. First, it is possible that in each case the amount of H_2S adsorbed was underestimated due to lag in the sensors. It is also possible there was residual H_2S inside the columns from previous experiments that caused inaccuracies in mass balance calculations. Finally, as previously discussed, the carbon used in these experiments was also found to produce sulfur-containing compounds upon heating. Compounds present in the carbon samples most likely contributed to the results found in this study.

The volume of gas that entered the GAC columns was compared to the volume of gas that left the columns during desorption to calculate the volume reduction ratio. This value serves as a metric for how well the gas was concentrated during the cyclic experiments. The results of these calculations also appear in Table 5.2.

Table 5.2: Thermal Regeneration Experimental Data

Date	**May 13**	**May 23**	**May 23**	**May 23**	**June 27**	**June 27**	**June 28**
Cycle Number (if applicable)	1	1	2	3	1	2	3
Recovery Percentage	83%	>100%	>100%	>100%	68%	69%	15%
Volume Reduction Ratio	10%	50%	65%	57%	61%	46%	71%

The overall average volume reduction ratio was 51 ± 19%, noting that there was one experiment on May 13 that had a notably lower value (10%). The likely reason for this was that air was pumped through the GAC columns in a less-efficient manner than other experiments. Typically, air was pumped through the columns after they were sufficiently heated. It is possible that the pumping time could have been reduced to improve this ratio. Without the outlier, the average becomes 58 ± 9%. This data indicates that a significant reduction in volume took place in most of the experiments; the gas became more concentrated through cyclic adsorption and desorption.

The final step of the odor control device is biological treatment. Over the course of the experiments, the treatment efficiency of the BTF during experiments at the landfill was poor. Initial tests showed promising results. Figure 5.8. shows results from an experiment where H_2S gas was passed directly through the BTF. This experiment showed clear evidence of some treatment by the biofilm. The treatment was verified by COD

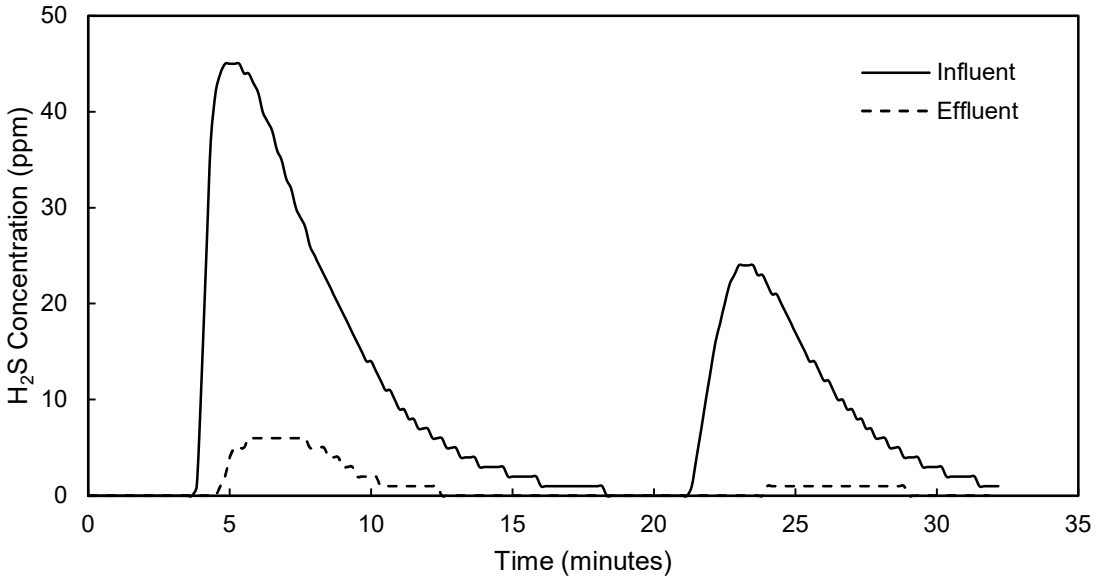

Figure 5.8: Initial BTF Results – H_2S added directly to BTF (April 21, 2022)

tests of the influent and effluent of the trickling solution in the BTF. In one experiment conducted shortly after start-up, the influent COD was 4,452 ± 36 mg/L and the effluent showed a value of 1,812 ± 9 mg/L. Nonetheless, subsequent experiments showed little to no treatment of H_2S based on data taken during various visits to the landfill. The COD of two samples taken later from the BTF showed a diminished removal of COD by the microbial consortium. The influent COD in this case was 4,902 ± 270 mg/L and the effluent was 4,306 ± 137 mg/L. This drastic difference in COD removal indicates that something had occurred which severely reduced the activity of the bacteria.

Several causes may explain this phenomenon. A possible explanation may have been that the biofilm had become overgrown and lost its ability to treat H_2S gas. To address this possibility, the BTF was backwashed to remove excess biomass that had accumulated inside. Subsequent testing showed little to no improvement in the treatment efficiency of the BTF. Another possibility is that the gas did not become adequately acclimated to H_2S during the start-up period. Regular amounts of H_2S were introduced to the BTF during the start-up process, but it possible that it was insufficient to sustain the biofilm over a long period of time. The organics present in the nutrient solution could have caused the biomass to become acclimated to the addition of organic compounds instead of H_2S. Furthermore, it is possible that the obtained sample of return activated sludge (RAS) did not contain enough sulfur-oxidizing bacteria (SOB). The absence of this bacteria would prevent the degradation of sulfur-containing compounds. Any SOB present in the original sample may have been weakened by competition with other microorganisms that fed on organics. One final likely cause of the BTF's poor performance is the temperature of the air that was introduced to the BTF during the

operation of the heated GAC columns. Though the temperature of the air was not taken during experimentation, it is expected that the air inside the columns may have been hot enough to adversely affect the biofilm during repeated exposure. For these reasons, there is a lack of extensive results from the biological treatment stage of the pilot device.

5.4. Summary

This chapter examined the construction and operation of pilot odor control device and discussed the results that were obtained during experimentation at the Loup Central Landfill. The first few stages of the device, namely the gas extraction system, the gas directional system, and the concentrator system provided favorable results. Evidence was provided for successful adsorption and desorption of H_2S via thermal regeneration. Additionally, the volume of H_2S-laden gas that exited the concentrator system was significantly smaller than the volume that entered the system. However, following concentration, the gas was not effectively treated by the BTF in the final stage. Despite some promising results early on, the bacteria failed to show consistent treatment of H_2S. The possible reasons for the lack of effective treatment were discussed. Further experimentation with a BTF would be necessary to determine the exact cause of these results and to identify a solution for addressing this issue.

CHAPTER 6: CONCLUSION

6.1. Summary of Findings

The primary objective of this work was to build and operate a pilot odor control device to investigate the feasibility of using an activated carbon (GAC) concentrator system to enhance the treatment efficiency of a biotrickling filter (BTF). Before building and testing the odor control device, cyclic adsorption and desorption experiments were conducted with various GACs to determine the adsorbent and conditions for use in the odor control device. The experiments demonstrated that thermal regeneration of GACs was feasible and effective, though the efficiency of regeneration appeared to decrease after more than one cycle. In the first cycle, the regeneration efficiency was approximately 70%, with each subsequent cycle showing roughly 50% efficiency. Furthermore, it was determined that heating the GAC to temperatures nearing 500°C was necessary to successfully regenerate it thereby producing concentrated H_2S gas.

The pilot odor control device was successfully constructed and installed at Loup Central Landfill. Operation lasted approximately three months between March and May 2022. Data obtained from the landfill gas showed that there was no measurable amount of H_2S in the gas emissions. Therefore, experimentation required the production of H_2S and subsequent addition to the raw landfill gas. Several experiments were run to test the individual components of the pilot odor control device. The activated carbon captured the incoming H_2S at an efficiency of roughly 75% (± 15%) and then regenerated at an overall efficiency of 76% (± 26%), noting that multiple cycles produced regeneration above 100% due to reasons explained previously. Results from the biotrickling filter initially

showed signs of degradation, and prolonged operation showed that it did not efficiently treat incoming H_2S.

6.2. Recommendations for Future Work

Initial testing at the Loup Central Landfill has concluded, so future testing may consist of visits to other sites in hopes of learning more about the application of this pilot odor control device. This technology has the potential for use in treating odors from municipal wastewater treatment and conveyance, and the hazardous air pollutants (HAPs) generated in ethanol production. It is also possible that this technology would provide benefits as a low-cost method for the preliminary removal of impurities in gas from landfills or anaerobic digestion. Impurities in this gas could be removed via GAC and treated with a BTF without diluting methane.

One of the lingering questions at the conclusion of this study is the reason for the lack of treatment by the BTF. Furthermore, the efficiency of the BTF was unsatisfactory and did not provide a satisfying conclusion to the treatment provided by the pilot odor control device. The poor performance could be the result of multiple possible factors, including insufficient time for the biomass to acclimate to the H_2S, an excessive buildup of biomass growing on support media, the H_2S-degrading bacteria being competitively weakened by bacteria that preferred organics or aerobic compounds, and excessive amounts of heat in the influent gas. It is likely that further experimentation may provide answers for these findings.

6.3. Recommendations for Modifications to Apparatus and Operation Methods

Further work with the pilot odor control device described in this thesis may be improved with a series of modifications to the apparatus and the methods used to operate it. These changes are described in the following list.

- The temperature of the gas entering the BTF may have played a role in reducing its activity. Some form of cooling is recommended to ensure that the air which enters the BTF does adversely affect the biofilm. Investigation of the temperature profile of the gas leaving the GAC columns during thermal regeneration is an essential task in determining an effective solution. Some suggestions to enact this change include:
    - The addition of cooler air leaving the GAC columns, though the H_2S would become less concentrated in this manner.
    - The addition of a heat exchanger or a cyclone. This modification will increase the residence time of the air inside the piping. A material that is non-corrosive is recommended (i.e. plastic or stainless steel).
    - The lengthening of piping between the BTF and the GAC columns to allow for more cooling while the air is transit.

- The addition of conduit to the wiring of the regeneration blower is necessary to ensure the safety of the person(s) when using it in the presence of landfill gas containing methane. Housing the wiring of the blower inside conduit prevents oxygen from entering the body of the motor, rendering it explosion-proof. Using the blower without conduit does not guarantee the user's safety.
- Increased monitoring of the biofilm in the BTF is one of the top priorities given the poor results that were documented in this work. It is recommended that regular observations of the influent and effluent be implemented to confirm the activity of the microorganisms. Suggestions for these observations include:
    - An analysis of the compounds in the BTF effluent with an emphasis on the presence of sulfates.
    - Measurements of the pH of both the influent and effluent, knowing that when H_2S is degraded by the biofilm, sulfuric acid is produced which lowers the pH. Regular additions of nutrient solution will provide a pathway for removing this byproduct, but the use of a buffer is recommended to maintain a constant pH within the system.
- If additional bench scale testing is conducted with GAC or another adsorbent based on the methods explained in Chapter 3, the mass flow controller needs to be placed before the reaction vessel. This adjustment will prevent corrosion inside the controller caused by repeated exposure to H_2S.

Further information concerning various issues that were encountered during operation of the pilot odor control device can be found in Appendix F along with methods for troubleshooting these issues.

REFERENCES

Adib, F., A. Bagreev, and T. J. Bandosz. 1999. "Effect of pH and Surface Chemistry on the Mechanism of H2S Removal by Activated Carbons." *Journal of Colloid and Interface Science*, 216 (2): 360–369. https://doi.org/10.1006/jcis.1999.6335.

Agilent. 2022. "490 MicroGC System." Santa Clara, CA.

Al Mamun, M. R. 2015. "Removal of Hydrogen Sulfide (H2S) from Biogas Using Zero-Valent Iron." *Journal of Clean Energy Technologies*, 3: 428–432. https://doi.org/10.7763/JOCET.2015.V3.236.

Alfonsín, C., R. Lebrero, J. M. Estrada, R. Muñoz, N. J. R. (Bart) Kraakman, G. Feijoo, and M. T. Moreira. 2015. "Selection of odour removal technologies in wastewater treatment plants: A guideline based on Life Cycle Assessment." *Journal of Environmental Management*, 149: 77–84. https://doi.org/10.1016/j.jenvman.2014.10.011.

Ania, C. O., J. A. Menéndez, J. B. Parra, and J. J. Pis. 2004. "Microwave-induced regeneration of activated carbons polluted with phenol. A comparison with conventional thermal regeneration." *Carbon*, 42 (7): 1383–1387. https://doi.org/10.1016/j.carbon.2004.01.010.

Bagreev, A., J. Angel Menendez, I. Dukhno, Y. Tarasenko, and T. J. Bandosz. 2004. "Bituminous coal-based activated carbons modified with nitrogen as adsorbents of hydrogen sulfide." *Carbon*, 42 (3): 469–476. https://doi.org/10.1016/j.carbon.2003.10.042.

Bagreev, A., S. Katikaneni, S. Parab, and T. J. Bandosz. 2005. "Desulfurization of digester gas: prediction of activated carbon bed performance at low concentrations of hydrogen sulfide." *Catalysis Today*, 99 (3): 329–337. https://doi.org/10.1016/j.cattod.2004.10.008.

Bagreev, A., H. Rahman, and T. J. Bandosz. 2000a. "Wood-Based Activated Carbons as Adsorbents of Hydrogen Sulfide: A Study of Adsorption and Water Regeneration Processes." *Ind. Eng. Chem. Res.*, 39 (10): 3849–3855. American Chemical Society. https://doi.org/10.1021/ie0004139.

Bagreev, A., H. Rahman, and T. J. Bandosz. 2000b. "Study of H2S Adsorption and Water Regeneration of Spent Coconut-Based Activated Carbon." *Environ. Sci. Technol.*, 34 (21): 4587–4592. American Chemical Society. https://doi.org/10.1021/es001150c.

Bagreev, A., H. Rahman, and T. J. Bandosz. 2001. "Thermal regeneration of a spent activated carbon previously used as hydrogen sulfide adsorbent." *Carbon*, 39 (9): 1319–1326. https://doi.org/10.1016/S0008-6223(00)00266-9.

Bagreev, A., H. Rahman, and T. J. Bandosz. 2002. "Study of regeneration of activated carbons used as H2S adsorbents in water treatment plants." *Advances in Environmental Research*, 6 (3): 303–311. https://doi.org/10.1016/S1093-0191(01)00063-6.

Balsamo, M., S. Cimino, G. de Falco, A. Erto, and L. Lisi. 2016. "ZnO-CuO supported on activated carbon for H2S removal at room temperature." *Chemical Engineering Journal*, 304: 399–407. https://doi.org/10.1016/j.cej.2016.06.085.

Bandosz, T. J. 1999. "Effect of pore structure and surface chemistry of virgin activated carbons on removal of hydrogen sulfide." *Carbon*, 37 (3): 483–491. https://doi.org/10.1016/S0008-6223(98)00217-6.

Bandosz, T. J. 2002. "On the Adsorption/Oxidation of Hydrogen Sulfide on Activated Carbons at Ambient Temperatures." *Journal of Colloid and Interface Science*, 246 (1): 1–20. https://doi.org/10.1006/jcis.2001.7952.

Benjamin, M. M., and D. F. Lawler. 2013. *Water Quality Engineering: Physical / Chemical Treatment Processes*. John Wiley & Sons.

Bruchet, A., V. Decottignies, and G. Filippi. 2009. "Effectiveness of masking agents: outcome of a three-year study at pilot and full scales." *Water science and technology*, 60 (1): 97–105. England. https://doi.org/10.2166/wst.2009.300.

Chiang, H.-L., J.-H. Tsai, C.-L. Tsai, and Y.-C. Hsu. 2000. "Adsorption characteristics of alkaline activated carbon exemplified by water vapor, H2S, and CH3SH gas." *Separation science and technology*, 35 (6): 903–918. Taylor & Francis.

Cohen, G. 2020. "Concentration and Treatment of Odors Generated by Landfills." *Civil and Environmental Engineering Theses, Dissertations, and Student Research*.

Coppola, G., and D. Papurello. 2019. "Biogas Cleaning: Activated Carbon Regeneration for H2S Removal." *Clean Technologies*, 1 (1). https://doi.org/10.3390/cleantechnol1010004.

Eun, S., D. R. Reinhart, C. D. Cooper, T. G. Townsend, and A. Faour. 2007. "Hydrogen sulfide flux measurements from construction and demolition debris (C&D) landfills." *Waste Management*, 27 (2): 220–227. https://doi.org/10.1016/j.wasman.2005.12.019.

Gabriel, D., and M. A. Deshusses. 2003. "Performance of a full-scale biotrickling filter treating H2S at a gas contact time of 1.6 to 2.2 seconds." *Environmental Progress*, 22 (2): 111–118. https://doi.org/10.1002/ep.670220213.

Gospodarek, M., P. Rybarczyk, B. Szulczyński, and J. Gębicki. 2019. "Comparative Evaluation of Selected Biological Methods for the Removal of Hydrophilic and Hydrophobic Odorous VOCs from Air." *Processes*, 7 (4): 187. Multidisciplinary Digital Publishing Institute. https://doi.org/10.3390/pr7040187.

Greene, E. A., C. Hubert, M. Nemati, G. E. Jenneman, and G. Voordouw. 2003. "Nitrite reductase activity of sulphate-reducing bacteria prevents their inhibition by nitrate-reducing, sulphide-oxidizing bacteria." *Environmental Microbiology*, 5 (7): 607–617. https://doi.org/10.1046/j.1462-2920.2003.00446.x.

Gutierrez, O., D. Park, K. R. Sharma, and Z. Yuan. 2009. “Effects of long-term pH elevation on the sulfate-reducing and methanogenic activities of anaerobic sewer biofilms.” *Water Research*, 43 (9): 2549–2557. https://doi.org/10.1016/j.watres.2009.03.008.

Henning, K.-D., and S. Schäfer. 1993. “Impregnated activated carbon for environmental protection.” *Gas Separation & Purification*, 7 (4): 235–240. https://doi.org/10.1016/0950-4214(93)80023-P.

Hu, L., Y. Du, and Y. Long. 2017. “Relationship between H2S emissions and the migration of sulfur-containing compounds in landfill sites.” *Ecological Engineering*, 106: 17–23. https://doi.org/10.1016/j.ecoleng.2017.05.026.

Huang, C.-C., C.-H. Chen, and S.-M. Chu. 2006. “Effect of moisture on H2S adsorption by copper impregnated activated carbon.” *Journal of Hazardous Materials*, 136 (3): 866–873. https://doi.org/10.1016/j.jhazmat.2006.01.025.

Kim, S., and M. A. Deshusses. 2005. “Understanding the limits of H2S degrading biotrickling filters using a differential biotrickling filter.” *Chemical Engineering Journal*, Selected papers from the USC-CSC-TRG Biofiltration Conference, October 2004, 113 (2): 119–126. https://doi.org/10.1016/j.cej.2005.05.001.

Ko, J. H., Q. Xu, and Y.-C. Jang. 2015. “Emissions and Control of Hydrogen Sulfide at Landfills: A Review.” *Critical Reviews in Environmental Science and Technology*, 45 (19): 2043–2083. Taylor & Francis. https://doi.org/10.1080/10643389.2015.1010427.

Kristjansson, J. K., and P. Schönheit. 1983. “Why Do Sulfate-Reducing Bacteria Outcompete Methanogenic Bacteria for Substrates?” *Oecologia*, 60 (2): 264–266. Springer.

Kushkevych, I., M. Vítězová, T. Vítěz, and M. Bartoš. 2017. “Production of biogas: relationship between methanogenic and sulfate-reducing microorganisms.” *Open Life Sciences*, 12 (1): 82–91. De Gruyter Open Access. https://doi.org/10.1515/biol-2017-0009.

Lee, S., Q. Xu, M. Booth, T. G. Townsend, P. Chadik, and G. Bitton. 2006. “Reduced sulfur compounds in gas from construction and demolition debris landfills.” *Waste Management*, 26 (5): 526–533. https://doi.org/10.1016/j.wasman.2005.10.010.

Letelier-Gordo, C. O., S. L. Aalto, S. Suurnäkki, and P. B. Pedersen. 2020. “Increased sulfate availability in saline water promotes hydrogen sulfide production in fish organic waste.” *Aquacultural Engineering*, 89: 102062. https://doi.org/10.1016/j.aquaeng.2020.102062.

Liu, J., J. Wang, N. Zhang, and H. Zhao. 2018. “On the explosion limit of syngas with CO2 and H2O additions.” *International Journal of Hydrogen Energy*, 43 (6): 3317–3329. https://doi.org/10.1016/j.ijhydene.2017.12.176.

Marsh, H., and F. R. Reinoso. 2006. *Activated Carbon*. Elsevier.

Muyzer, G., and A. J. M. Stams. 2008. “The ecology and biotechnology of sulphate-reducing bacteria.” *Nat Rev Microbiol*, 6 (6): 441–454. Nature Publishing Group. https://doi.org/10.1038/nrmicro1892.

NAGATA, Y. 1990. “Measurement of Odor Threshold by Triangle Odor Bag Method.” *Bull. Japan Environmental Sanitation Center*, 17: 77–89.

Nakamura, T., S. Tanada, N. Kawasaki, T. Hara, J. Fujisawa, and K. Shibata. 1996. “Hydrogen sulfide removal by iron containing activated carbon.” *null*, 55 (1–4): 279–283. Taylor & Francis. https://doi.org/10.1080/02772249609358343.

O’Flaherty, V., T. Mahony, R. O’Kennedy, and E. Colleran. 1998. “Effect of pH on growth kinetics and sulphide toxicity thresholds of a range of methanogenic, syntrophic and sulphate-reducing bacteria.” *Process Biochemistry*, 33 (5): 555–569. https://doi.org/10.1016/S0032-9592(98)00018-1.

Omar, H., and S. Rohani. 2015. “Treatment of landfill waste, leachate and landfill gas: A review.” *Front. Chem. Sci. Eng.*, 9 (1): 15–32. https://doi.org/10.1007/s11705-015-1501-y.

Salvador, F., and C. S. Jiménez. 1996. “A new method for regenerating activated carbon by thermal desorption with liquid water under subcritical conditions.” *Carbon*, 34 (4): 511–516. https://doi.org/10.1016/0008-6223(95)00211-1.

Singh, K. P., A. Malik, S. Sinha, and P. Ojha. 2008. “Liquid-phase adsorption of phenols using activated carbons derived from agricultural waste material.” *Journal of Hazardous Materials*, 150 (3): 626–641. https://doi.org/10.1016/j.jhazmat.2007.05.017.

Sitthikhankaew, R., S. Predapitakkun, R. (Wibulswas) Kiattikomol, S. Pumhiran, S. Assabumrungrat, and N. Laosiripojana. 2011. “Comparative Study of Hydrogen Sulfide Adsorption by using Alkaline Impregnated Activated Carbons for Hot Fuel Gas Purification.” *Energy Procedia*, 9th Eco-Energy and Materials Science and Engineering Symposium, 9: 15–24. https://doi.org/10.1016/j.egypro.2011.09.003.

Tansel, B., and B. Inanloo. 2019. “Odor impact zones around landfills: Delineation based on atmospheric conditions and land use characteristics.” *Waste Management*, 88: 39–47. https://doi.org/10.1016/j.wasman.2019.03.028.

US EPA, O. 2017. “National Overview: Facts and Figures on Materials, Wastes and Recycling.” Overviews and Factsheets. Accessed September 12, 2021. https://www.epa.gov/facts-and-figures-about-materials-waste-and-recycling/national-overview-facts-and-figures-materials.

Wang, S., H. Nam, and H. Nam. 2020. “Preparation of activated carbon from peanut shell with KOH activation and its application for H2S adsorption in confined space.” *Journal of Environmental Chemical Engineering*, 8 (2): 103683. https://doi.org/10.1016/j.jece.2020.103683.

Weimann, K., C. Adam, M. Buchert, and J. Sutter. 2021. “Environmental Evaluation of Gypsum Plasterboard Recycling.” *Minerals*, 11 (2): 101. Multidisciplinary Digital Publishing Institute. https://doi.org/10.3390/min11020101.

Xu, Q., and T. Townsend. 2014. “Factors affecting temporal H2S emission at construction and demolition (C&D) debris landfills.” *Chemosphere*, 96: 105–111. https://doi.org/10.1016/j.chemosphere.2013.07.052.

Xu, Q., T. Townsend, and G. Bitton. 2011. “Inhibition of hydrogen sulfide generation from disposed gypsum drywall using chemical inhibitors.” *Journal of Hazardous Materials*, 191 (1): 204–211. https://doi.org/10.1016/j.jhazmat.2011.04.063.

Xu, Q., T. Townsend, and D. Reinhart. 2010. “Attenuation of hydrogen sulfide at construction and demolition debris landfills using alternative cover materials.” *Waste Management*, 30 (4): 660–666. https://doi.org/10.1016/j.wasman.2009.10.022.

Yan, R., T. Chin, Y. L. Ng, H. Duan, D. T. Liang, and J. H. Tay. 2004. “Influence of Surface Properties on the Mechanism of H2S Removal by Alkaline Activated Carbons.” *Environ. Sci. Technol.*, 38 (1): 316–323. American Chemical Society. https://doi.org/10.1021/es0303992.

Yang, K., Q. Xu, T. G. Townsend, P. Chadik, G. Bitton, and M. Booth. 2006. “Hydrogen Sulfide Generation in Simulated Construction and Demolition Debris Landfills: Impact of Waste Composition.” *Journal of the Air & Waste Management Association*, 56 (8): 1130–1138. Taylor & Francis. https://doi.org/10.1080/10473289.2006.10464544.

Zhang, J., B. Dubey, and T. Townsend. 2014. “Effect of Moisture Control and Air Venting on H2S Production and Leachate Quality in Mature C&D Debris Landfills.” *Environ. Sci. Technol.*, 48 (20): 11777–11786. American Chemical Society. https://doi.org/10.1021/es5010957.

Zhang, J., H. Kim, B. Dubey, and T. Townsend. 2017. “Arsenic leaching and speciation in C&D debris landfills and the relationship with gypsum drywall content.” *Waste Management*, 59: 324–329. https://doi.org/10.1016/j.wasman.2016.10.023.

Zhou, W., X. Meng, J. Gao, H. Zhao, G. Zhao, and J. Ma. 2021. “Electrochemical regeneration of carbon-based adsorbents: a review of regeneration mechanisms, reactors, and future prospects.” *Chemical Engineering Journal Advances*, 5: 100083. https://doi.org/10.1016/j.ceja.2020.100083.

APPENDIX A: ODOR CONTROL DEVICE PARTS LIST

Table A.1: List of Parts in Gas Extraction System

Part	Description	Quantity
Blower	AMETEK Rotron EN101 regenerative blower, 0.5 HP	1
Cap	4” PVC cleanout plug	1
Piping	1” PVC, various lengths	1
Pipe Elbows	1” PVC 90-degree elbows	2

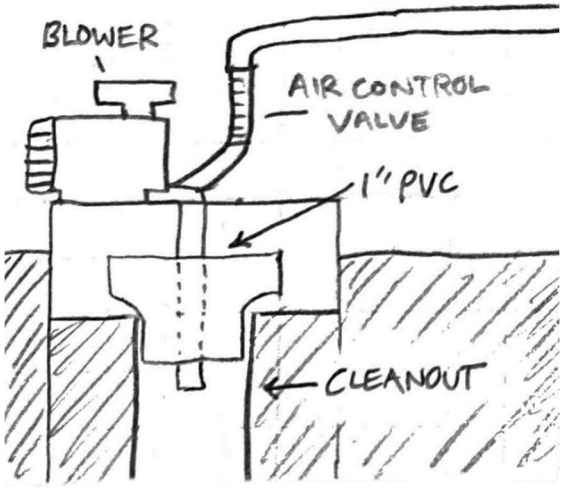

Figure A.1: Drawing of Gas Extraction System

Table A.2: List of Parts in Gas Transport System

Part	Description	Quantity
N/O Solenoids	1” 110 VAC Stainless Steel Solenoid Valve, Normally Open	2
N/C Solenoids	1” 110 VAC Stainless Steel Solenoid Valve, Normally Open	2
Controller	Orbit B-hyve Smart 12-Zone Sprinkler Controller	1
Transformer	110VAC/24VAC Transformer	1
Enclosure	Outdoor enclosure for transformer	1
Relay	24VAC 8-pin relay	1
Wire	12 gage wire, various lengths	1
Wire Nuts	Nuts for 12 gage wire	12
Piping	1” PVC, various lengths; 1” Stainless Steel, various lengths	1
Pipe Elbows	1” PVC 90-degree elbows	10
Union Fittings	1” PVC union fittings; 1” Stainless Steel, various lengths	4
Check Valves	1” Swing-type check valves, stainless steel	3

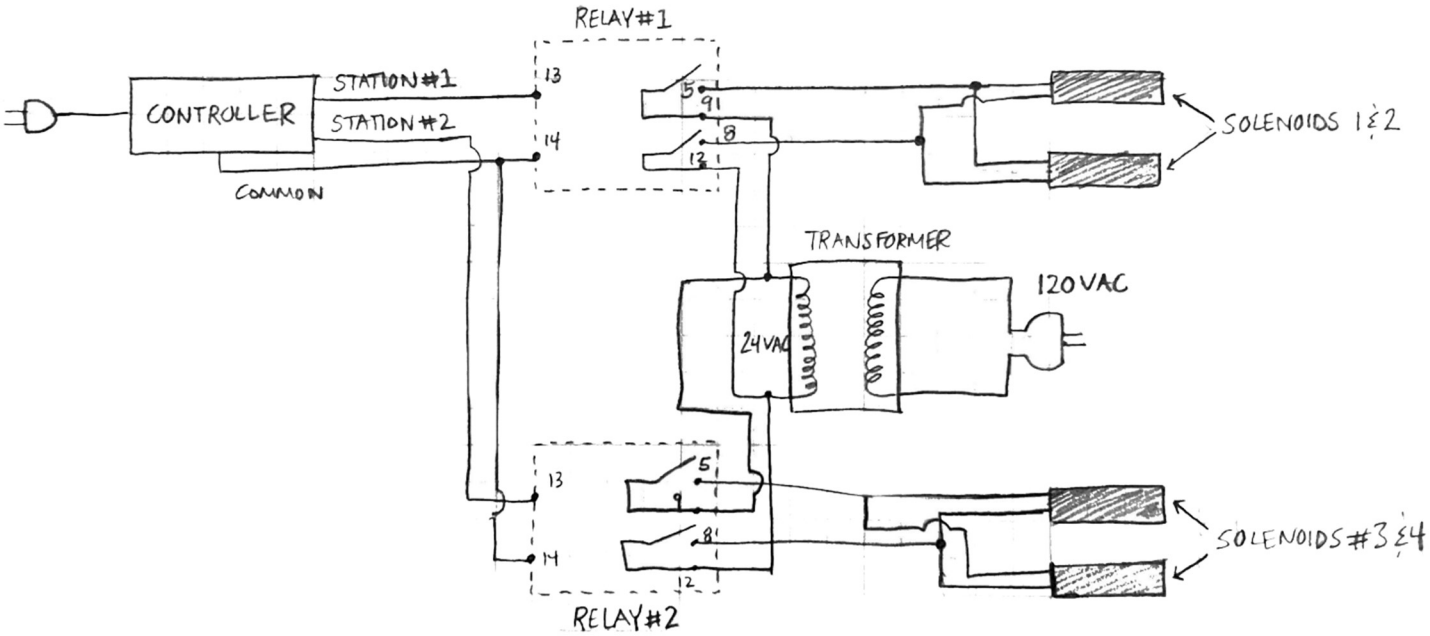

Figure A.2: Wiring Diagram for Gas Transport System

Table A.3: List of Parts in Gas Concentrator System

Part	Description	Quantity
Columns	18” Black Steel Pipes, 1” Diameter	2
Air Pump	GAST Air Compressor	1
Activated Carbon	GC Sulfursorb Plus (General Carbon), roughly 20 g per column	1
Gravel	Pea gravel for supporting carbon	
Heat Tape	Briskheat High-Wattage Insulated Heat Tape, 2’ length	1
Thermocouple	K-type thermocouple	2
Insulation	High-temperature fiberglass insulation	1
Straps	Pipe straps for securing heat tape and insulation to pipes	4
Cross	1/4” stainless steel cross fitting	2
Reducing Coupling	1-1/4” stainless steel reducing adapter	4
Timer	120 VAC timer box with independently wired outlets	2

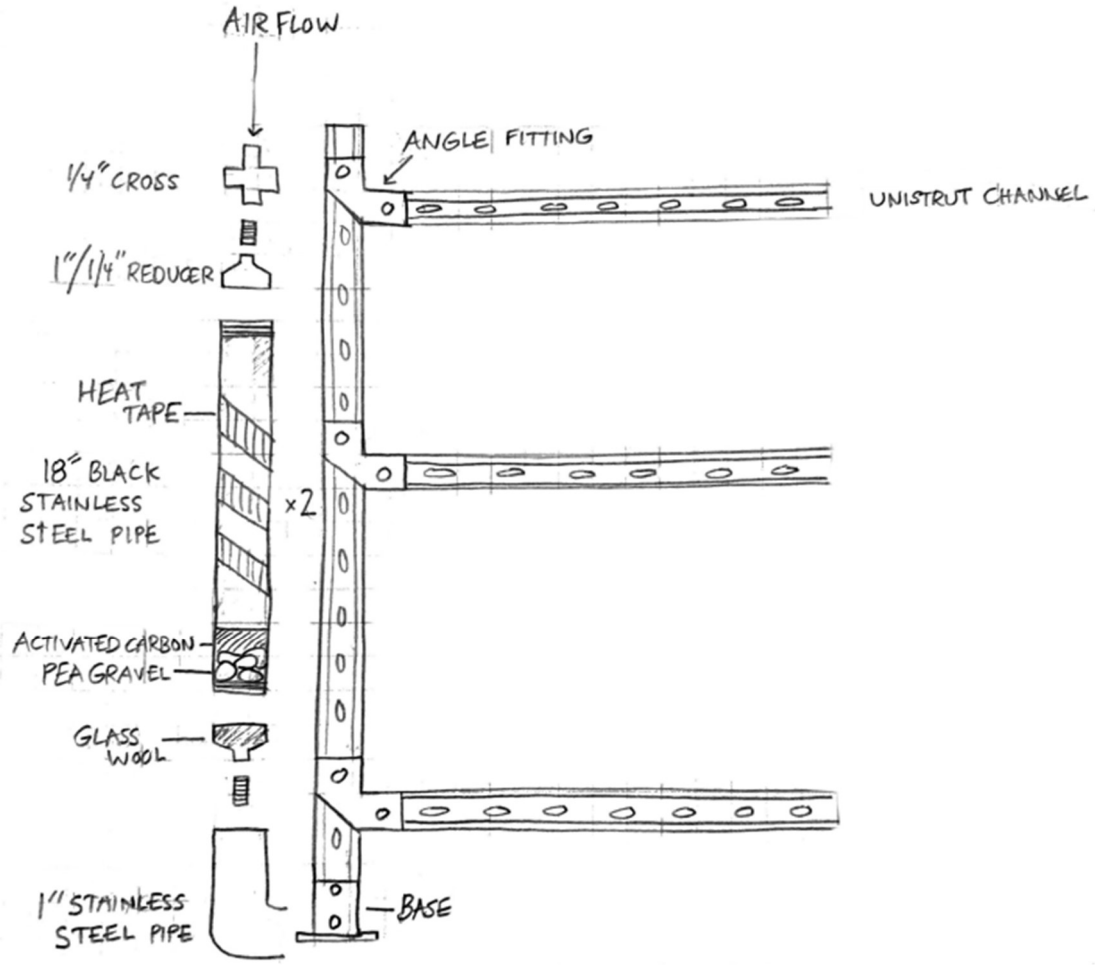

Figure A.3: Drawing of Activated Carbon Column

Table A.4: List of Parts in Biological Trickling Filter

Part	Description	Quantity
Columns	4” PVC, 5’ in length	2
Caps	4” PVC pipe cap	1
Tubing	1/2” plastic tubing, various lengths	1
Nozzle	1/4” nozzle	2
Sample ports	1/2” push to connect tubing fittings	4
Pump	FMI Fluid Lab Metering Pump	1
Media	MATALA High Density Filter Media, roughly 1 ft^3	1
Buckets	Nutrient solution storage and effluent collection	2

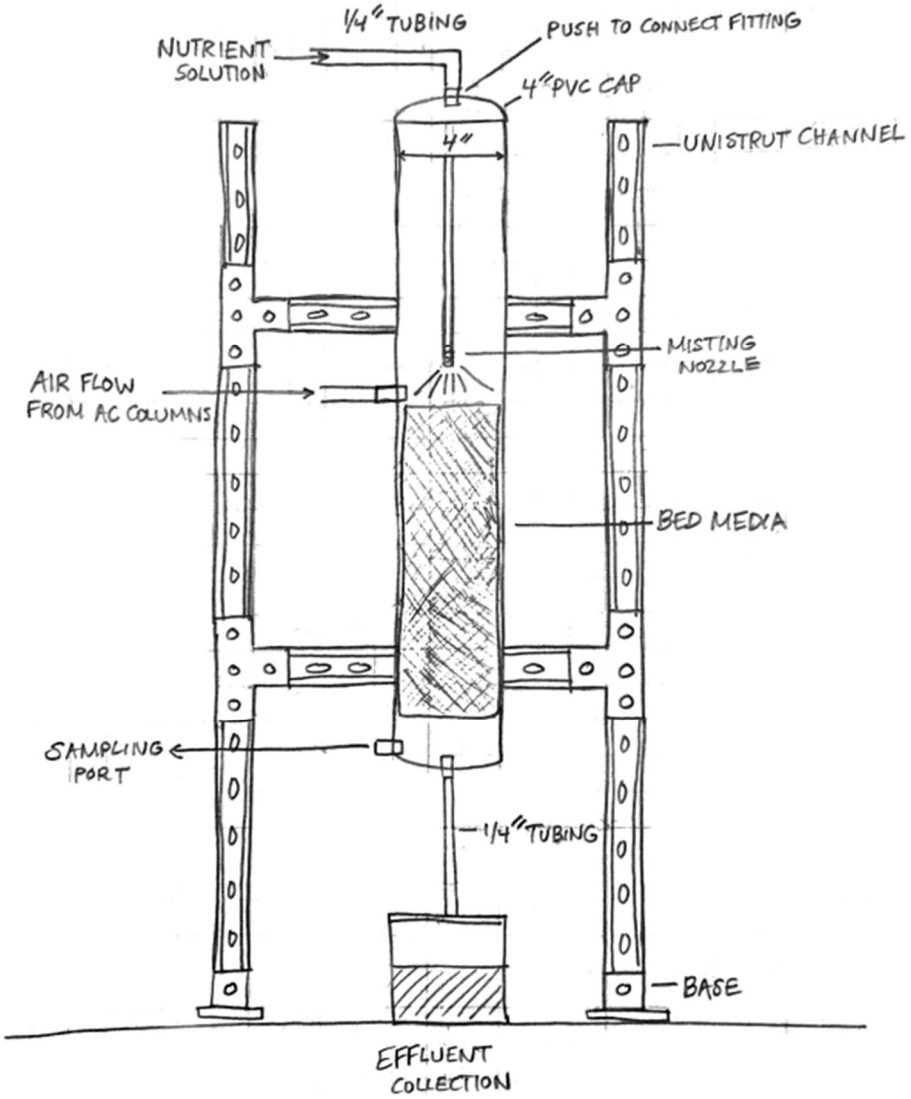

Figure A.4: Drawing of Biotrickling Filter

Table A.5: List of Parts in Sampling System

Part	Description	Quantity
Sampler	DETECTION INSTRUMENTS sampling system	1
Sensors	ACRULOG PPM H_2S Loggers	2
Sample Line	1/4” Tubing, various lengths	1

APPENDIX B: PILOT DEVICE OPERATING DATA

Table B.1: Adsorption Data from May 23, 2022

Time Stamp	Temp. (°F)	Humidity (%)	H2S (PPM) – GAC Inlet	H2S (PPM) – GAC Outlet
5/23/2022, 1:08:02 PM	71.6	36.3	0	0
5/23/2022, 1:08:12 PM	71.6	36.3	0	0
5/23/2022, 1:08:22 PM	71.6	36.3	0	0
5/23/2022, 1:08:32 PM	71.4	36.3	0	0
5/23/2022, 1:08:42 PM	71.6	36.3	0	0
5/23/2022, 1:08:52 PM	71.6	36.3	0	0
5/23/2022, 1:09:02 PM	71.6	36.3	0	0
5/23/2022, 1:09:12 PM	71.6	36.3	0	0
5/23/2022, 1:09:22 PM	71.6	36.3	0	0
5/23/2022, 1:09:32 PM	71.4	36.3	0	0
5/23/2022, 1:09:42 PM	71.4	36.3	0	0
5/23/2022, 1:09:52 PM	71.4	36.3	0	0
5/23/2022, 1:10:02 PM	71.4	36.2	0	0
5/23/2022, 1:10:12 PM	71.4	36.2	0	0
5/23/2022, 1:10:22 PM	71.2	36.2	0	0
5/23/2022, 1:10:32 PM	71.2	36.2	0	0
5/23/2022, 1:10:42 PM	71.2	36.2	0	0
5/23/2022, 1:10:52 PM	71.2	36.2	0	0
5/23/2022, 1:11:02 PM	71.2	36.2	0	0
5/23/2022, 1:11:12 PM	71.1	36.2	0	0
5/23/2022, 1:11:22 PM	71.1	36.2	0	0
5/23/2022, 1:11:32 PM	71.1	36.2	0	0
5/23/2022, 1:11:42 PM	71.1	36.2	0	0
5/23/2022, 1:11:52 PM	70.9	36.2	0	0
5/23/2022, 1:12:02 PM	70.9	36.2	0	0
5/23/2022, 1:12:12 PM	70.9	36.2	0	0
5/23/2022, 1:12:22 PM	70.9	36.2	0	0
5/23/2022, 1:12:32 PM	70.9	36.2	0	0
5/23/2022, 1:12:42 PM	70.7	36.2	0	0
5/23/2022, 1:12:52 PM	70.7	36.3	0	0
5/23/2022, 1:13:02 PM	70.7	36.2	0	0
5/23/2022, 1:13:12 PM	70.7	36.3	0	0
5/23/2022, 1:13:22 PM	70.7	36.3	0	0
5/23/2022, 1:13:32 PM	70.5	36.3	0	0

5/23/2022, 1:13:42 PM	70.5	36.3	0	0
5/23/2022, 1:13:52 PM	70.5	36.3	0	0
5/23/2022, 1:14:02 PM	70.5	36.3	0	0
5/23/2022, 1:14:12 PM	70.5	36.3	0	0
5/23/2022, 1:14:22 PM	70.3	36.3	0	0
5/23/2022, 1:14:32 PM	70.3	36.3	0	0
5/23/2022, 1:14:42 PM	70.3	36.3	0	0
5/23/2022, 1:14:52 PM	70.3	36.3	0	0
5/23/2022, 1:15:02 PM	70.3	36.3	0	0
5/23/2022, 1:15:12 PM	70.2	36.3	0	0
5/23/2022, 1:15:22 PM	70.2	36.3	0	0
5/23/2022, 1:15:32 PM	70.2	36.3	0	0
5/23/2022, 1:15:42 PM	70.2	36.2	0	0
5/23/2022, 1:15:52 PM	70	36.2	0	0
5/23/2022, 1:16:02 PM	70	36.2	0	0
5/23/2022, 1:16:12 PM	70	36.2	0	0
5/23/2022, 1:16:22 PM	70	36.2	0	0
5/23/2022, 1:16:32 PM	70	36.2	0	0
5/23/2022, 1:16:42 PM	69.8	36.2	0	0
5/23/2022, 1:16:52 PM	69.8	36.2	7	2
5/23/2022, 1:17:02 PM	69.8	36.2	20	8
5/23/2022, 1:17:12 PM	69.8	36.2	28	12
5/23/2022, 1:17:22 PM	69.6	36.2	35	16
5/23/2022, 1:17:32 PM	69.6	36.2	40	19
5/23/2022, 1:17:42 PM	69.6	36.2	44	21
5/23/2022, 1:17:52 PM	69.6	36.2	48	23
5/23/2022, 1:18:02 PM	69.6	36.2	50	24
5/23/2022, 1:18:12 PM	69.4	36.1	51	24
5/23/2022, 1:18:22 PM	69.4	36.1	51	25
5/23/2022, 1:18:32 PM	69.4	36.1	51	24
5/23/2022, 1:18:42 PM	69.3	36.1	50	24
5/23/2022, 1:18:52 PM	69.3	36.1	49	23
5/23/2022, 1:19:02 PM	69.3	36.1	48	23
5/23/2022, 1:19:12 PM	69.3	36.1	46	22
5/23/2022, 1:19:22 PM	69.3	36.1	45	21
5/23/2022, 1:19:32 PM	69.1	36.1	43	20
5/23/2022, 1:19:42 PM	69.1	36.1	41	19
5/23/2022, 1:19:52 PM	69.1	36.1	39	18
5/23/2022, 1:20:02 PM	69.1	36.1	37	17
5/23/2022, 1:20:12 PM	68.9	36.1	35	16
5/23/2022, 1:20:22 PM	68.9	36.1	32	15

5/23/2022, 1:20:32 PM	68.9	36.1	30	14
5/23/2022, 1:20:42 PM	68.9	36.1	29	13
5/23/2022, 1:20:52 PM	68.9	36.1	27	12
5/23/2022, 1:21:02 PM	68.7	36.1	25	11
5/23/2022, 1:21:12 PM	68.7	36.1	24	10
5/23/2022, 1:21:22 PM	68.7	36.1	22	10
5/23/2022, 1:21:32 PM	68.7	36.1	21	9
5/23/2022, 1:21:42 PM	68.5	36.1	19	8
5/23/2022, 1:21:52 PM	68.5	36.1	18	8
5/23/2022, 1:22:02 PM	68.5	36.1	17	7
5/23/2022, 1:22:12 PM	68.5	36.1	16	7
5/23/2022, 1:22:22 PM	68.5	36.1	14	6
5/23/2022, 1:22:32 PM	68.4	36.1	13	6
5/23/2022, 1:22:42 PM	68.4	36.1	12	5
5/23/2022, 1:22:52 PM	68.4	36.1	12	5
5/23/2022, 1:23:02 PM	68.4	36.1	11	4
5/23/2022, 1:23:12 PM	68.4	36.1	10	4
5/23/2022, 1:23:22 PM	68.2	36.1	9	4
5/23/2022, 1:23:32 PM	68.2	36.1	9	3
5/23/2022, 1:23:42 PM	68.2	36.1	8	3
5/23/2022, 1:23:52 PM	68.2	36.1	8	3
5/23/2022, 1:24:02 PM	68.2	36.1	7	3
5/23/2022, 1:24:12 PM	68	36.1	6	2
5/23/2022, 1:24:22 PM	68	36.1	6	2
5/23/2022, 1:24:32 PM	68	36.1	6	2
5/23/2022, 1:24:42 PM	68	36.1	5	2
5/23/2022, 1:24:52 PM	68	36.1	5	2
5/23/2022, 1:25:02 PM	68	36.1	4	2
5/23/2022, 1:25:12 PM	68	36.1	4	1
5/23/2022, 1:25:22 PM	67.8	36.1	4	1
5/23/2022, 1:25:32 PM	67.8	36.1	4	1
5/23/2022, 1:25:42 PM	67.8	36.1	3	1
5/23/2022, 1:25:52 PM	67.8	36.1	3	1
5/23/2022, 1:26:02 PM	67.8	36.2	3	1
5/23/2022, 1:26:12 PM	67.8	36.2	3	1
5/23/2022, 1:26:22 PM	67.8	36.2	2	1
5/23/2022, 1:26:32 PM	67.6	36.2	2	1
5/23/2022, 1:26:42 PM	67.6	36.2	2	0
5/23/2022, 1:26:52 PM	67.6	36.2	2	0
5/23/2022, 1:27:02 PM	67.6	36.2	2	0
5/23/2022, 1:27:12 PM	67.6	36.2	2	0

5/23/2022, 1:27:22 PM	67.6	36.2	1	0
5/23/2022, 1:27:32 PM	67.5	36.2	1	0
5/23/2022, 1:27:42 PM	67.5	36.2	1	0
5/23/2022, 1:27:52 PM	67.5	36.2	1	0
5/23/2022, 1:28:02 PM	67.5	36.2	1	0
5/23/2022, 1:28:12 PM	67.5	36.3	1	0
5/23/2022, 1:28:22 PM	67.5	36.3	1	0
5/23/2022, 1:28:32 PM	67.5	36.3	2	0
5/23/2022, 1:28:42 PM	67.5	36.3	6	3
5/23/2022, 1:28:52 PM	67.3	36.3	13	6
5/23/2022, 1:29:02 PM	67.3	36.3	21	10
5/23/2022, 1:29:12 PM	67.3	36.2	29	14
5/23/2022, 1:29:22 PM	67.3	36.3	37	19
5/23/2022, 1:29:32 PM	67.3	36.3	45	23
5/23/2022, 1:29:42 PM	67.3	36.3	53	27
5/23/2022, 1:29:52 PM	67.1	36.3	60	31
5/23/2022, 1:30:02 PM	67.1	36.3	66	34
5/23/2022, 1:30:12 PM	67.1	36.3	72	37
5/23/2022, 1:30:22 PM	67.1	36.3	76	39
5/23/2022, 1:30:32 PM	67.1	36.3	79	40
5/23/2022, 1:30:42 PM	67.1	36.3	80	41
5/23/2022, 1:30:52 PM	66.9	36.3	81	41
5/23/2022, 1:31:02 PM	66.9	36.3	80	40
5/23/2022, 1:31:12 PM	66.7	36.4	78	39
5/23/2022, 1:31:22 PM	66.7	36.4	76	38
5/23/2022, 1:31:32 PM	66.7	36.4	73	36
5/23/2022, 1:31:42 PM	66.7	36.4	70	34
5/23/2022, 1:31:52 PM	66.7	36.4	67	33
5/23/2022, 1:32:02 PM	66.7	36.4	64	31
5/23/2022, 1:32:12 PM	66.7	36.4	60	29
5/23/2022, 1:32:22 PM	66.7	36.5	57	27
5/23/2022, 1:32:32 PM	66.7	36.5	53	25
5/23/2022, 1:32:42 PM	66.7	36.5	50	23
5/23/2022, 1:32:52 PM	66.7	36.5	47	22
5/23/2022, 1:33:02 PM	66.7	36.6	44	20
5/23/2022, 1:33:12 PM	66.7	36.6	41	19
5/23/2022, 1:33:22 PM	66.7	36.6	38	17
5/23/2022, 1:33:32 PM	66.7	36.6	35	16
5/23/2022, 1:33:42 PM	66.7	36.6	33	15
5/23/2022, 1:33:52 PM	66.7	36.6	30	14
5/23/2022, 1:34:02 PM	66.6	36.7	28	13

5/23/2022, 1:34:12 PM	66.6	36.7	26	12
5/23/2022, 1:34:22 PM	66.6	36.7	24	11
5/23/2022, 1:34:32 PM	66.6	36.7	22	10
5/23/2022, 1:34:42 PM	66.6	36.7	21	9
5/23/2022, 1:34:52 PM	66.4	36.7	19	8
5/23/2022, 1:35:02 PM	66.4	36.8	18	8
5/23/2022, 1:35:12 PM	66.4	36.8	16	7
5/23/2022, 1:35:22 PM	66.4	36.8	15	7
5/23/2022, 1:35:32 PM	66.4	36.8	14	6
5/23/2022, 1:35:42 PM	66.4	36.8	13	6
5/23/2022, 1:35:52 PM	66.4	36.8	12	5
5/23/2022, 1:36:02 PM	66.2	36.8	11	5
5/23/2022, 1:36:12 PM	66.2	36.8	10	4
5/23/2022, 1:36:22 PM	66.2	36.8	10	4
5/23/2022, 1:36:32 PM	66.2	36.8	9	4
5/23/2022, 1:36:42 PM	66.2	36.9	8	3
5/23/2022, 1:36:52 PM	66.2	36.9	8	3
5/23/2022, 1:37:02 PM	66.2	36.9	7	3
5/23/2022, 1:37:12 PM	66.2	36.9	6	3
5/23/2022, 1:37:22 PM	66	36.9	6	2
5/23/2022, 1:37:32 PM	66	37	5	2
5/23/2022, 1:37:42 PM	66	37	5	2
5/23/2022, 1:37:52 PM	66	37	5	2
5/23/2022, 1:38:02 PM	66	37	4	2
5/23/2022, 1:38:12 PM	66	37	4	2
5/23/2022, 1:38:22 PM	66	37	4	1
5/23/2022, 1:38:32 PM	66	37.1	3	1
5/23/2022, 1:38:42 PM	66	37.1	3	1
5/23/2022, 1:38:52 PM	66	37.1	3	1
5/23/2022, 1:39:02 PM	65.8	37.1	3	1
5/23/2022, 1:39:12 PM	65.8	37.1	2	1
5/23/2022, 1:39:22 PM	65.8	37.1	2	1
5/23/2022, 1:39:32 PM	65.8	37.1	2	1
5/23/2022, 1:39:42 PM	65.8	37.1	2	1
5/23/2022, 1:39:52 PM	65.8	37.2	2	0
5/23/2022, 1:40:02 PM	65.8	37.2	2	0
5/23/2022, 1:40:12 PM	65.8	37.2	2	0
5/23/2022, 1:40:22 PM	65.8	37.2	1	0
5/23/2022, 1:40:32 PM	65.8	37.2	1	0
5/23/2022, 1:40:42 PM	65.7	37.2	1	0
5/23/2022, 1:40:52 PM	65.7	37.2	1	0

5/23/2022, 1:41:02 PM	65.7	37.2	1	0
5/23/2022, 1:41:12 PM	65.7	37.2	1	0
5/23/2022, 1:41:22 PM	65.7	37.2	1	0
5/23/2022, 1:41:32 PM	65.7	37.2	1	0
5/23/2022, 1:41:42 PM	65.7	37.2	1	0
5/23/2022, 1:41:52 PM	65.7	37.2	1	0
5/23/2022, 1:42:02 PM	65.7	37.2	1	0
5/23/2022, 1:42:12 PM	65.7	37.2	1	0
5/23/2022, 1:42:22 PM	65.7	37.2	1	0
5/23/2022, 1:42:32 PM	65.7	37.2	1	0
5/23/2022, 1:42:42 PM	65.5	37.2	0	0
5/23/2022, 1:42:52 PM	65.5	37.2	0	0
5/23/2022, 1:43:02 PM	65.5	37.2	0	0
5/23/2022, 1:43:12 PM	65.5	37.2	0	0
5/23/2022, 1:43:22 PM	65.5	37.3	0	0
5/23/2022, 1:43:32 PM	65.5	37.3	0	0
5/23/2022, 1:43:42 PM	65.5	37.2	0	0
5/23/2022, 1:43:52 PM	65.5	37.2	0	0
5/23/2022, 1:44:02 PM	65.5	37.2	0	0
5/23/2022, 1:44:12 PM	65.5	37.2	0	0

Table B.2: Desorption Data from May 23, 2022

Time Stamp	Temp. (°C)	Humidity (%)	H2S (PPM) – GAC Outlet	H2S (PPM) – BTF Outlet
5/23/2022, 3:48:06 PM	18.4	40.6	0	0
5/23/2022, 3:48:16 PM	18.4	40.6	0	0
5/23/2022, 3:48:26 PM	18.4	40.7	0	0
5/23/2022, 3:48:36 PM	18.4	40.7	0	0
5/23/2022, 3:48:46 PM	18.4	40.7	0	0
5/23/2022, 3:48:56 PM	18.4	40.7	0	0
5/23/2022, 3:49:06 PM	18.4	40.7	0	0
5/23/2022, 3:49:16 PM	18.4	40.7	0	0
5/23/2022, 3:49:26 PM	18.4	40.7	0	0
5/23/2022, 3:49:36 PM	18.4	40.8	0	0
5/23/2022, 3:49:46 PM	18.4	40.8	0	0
5/23/2022, 3:49:56 PM	18.4	40.8	0	0
5/23/2022, 3:50:06 PM	18.4	40.8	0	0
5/23/2022, 3:50:16 PM	18.4	40.8	0	0
5/23/2022, 3:50:26 PM	18.4	40.8	0	0

5/23/2022, 3:50:36 PM	18.4	40.9	0	0
5/23/2022, 3:50:46 PM	18.4	40.9	0	0
5/23/2022, 3:50:56 PM	18.4	40.9	0	0
5/23/2022, 3:51:06 PM	18.4	40.9	0	0
5/23/2022, 3:51:16 PM	18.4	40.9	0	0
5/23/2022, 3:51:26 PM	18.4	40.9	0	0
5/23/2022, 3:51:36 PM	18.4	40.9	0	0
5/23/2022, 3:51:46 PM	18.4	41	0	0
5/23/2022, 3:51:56 PM	18.4	41	0	0
5/23/2022, 3:52:06 PM	18.3	41	0	0
5/23/2022, 3:52:16 PM	18.3	41	0	0
5/23/2022, 3:52:26 PM	18.3	41.1	0	0
5/23/2022, 3:52:36 PM	18.3	41	0	0
5/23/2022, 3:52:46 PM	18.3	41.1	0	0
5/23/2022, 3:52:56 PM	18.3	41.1	0	0
5/23/2022, 3:53:06 PM	18.3	41.1	0	0
5/23/2022, 3:53:16 PM	18.3	41.1	0	0
5/23/2022, 3:53:26 PM	18.3	41.1	0	0
5/23/2022, 3:53:36 PM	18.3	41.1	0	0
5/23/2022, 3:53:46 PM	18.3	41.1	0	0
5/23/2022, 3:53:56 PM	18.3	41.2	0	0
5/23/2022, 3:54:06 PM	18.3	41.2	0	0
5/23/2022, 3:54:16 PM	18.3	41.2	0	0
5/23/2022, 3:54:26 PM	18.3	41.2	0	0
5/23/2022, 3:54:36 PM	18.3	41.2	4	0
5/23/2022, 3:54:46 PM	18.3	41.3	13	0
5/23/2022, 3:54:56 PM	18.3	41.3	22	0
5/23/2022, 3:55:06 PM	18.3	41.3	28	0
5/23/2022, 3:55:16 PM	18.3	41.3	33	0
5/23/2022, 3:55:26 PM	18.3	41.3	37	0
5/23/2022, 3:55:36 PM	18.3	41.4	40	0
5/23/2022, 3:55:46 PM	18.3	41.4	42	1
5/23/2022, 3:55:56 PM	18.3	41.4	44	5
5/23/2022, 3:56:06 PM	18.3	41.4	46	10
5/23/2022, 3:56:16 PM	18.3	41.4	47	18
5/23/2022, 3:56:26 PM	18.3	41.5	48	26
5/23/2022, 3:56:36 PM	18.3	41.5	49	34
5/23/2022, 3:56:46 PM	18.3	41.5	49	41
5/23/2022, 3:56:56 PM	18.3	41.5	49	46
5/23/2022, 3:57:06 PM	18.3	41.6	49	51
5/23/2022, 3:57:16 PM	18.3	41.6	48	55

5/23/2022, 3:57:26 PM	18.2	41.7	48	58
5/23/2022, 3:57:36 PM	18.2	41.7	47	60
5/23/2022, 3:57:46 PM	18.2	41.7	47	62
5/23/2022, 3:57:56 PM	18.2	41.7	46	64
5/23/2022, 3:58:06 PM	18.2	41.8	46	65
5/23/2022, 3:58:16 PM	18.2	41.8	46	65
5/23/2022, 3:58:26 PM	18.2	41.8	45	66
5/23/2022, 3:58:36 PM	18.2	41.8	45	66
5/23/2022, 3:58:46 PM	18.2	41.9	45	66
5/23/2022, 3:58:56 PM	18.2	41.9	45	66
5/23/2022, 3:59:06 PM	18.2	41.9	44	66
5/23/2022, 3:59:16 PM	18.2	42	44	66
5/23/2022, 3:59:26 PM	18.2	42	44	66
5/23/2022, 3:59:36 PM	18.2	42	43	65
5/23/2022, 3:59:46 PM	18.2	42	43	65
5/23/2022, 3:59:56 PM	18.2	42.1	42	65
5/23/2022, 4:00:06 PM	18.2	42.1	42	65
5/23/2022, 4:00:16 PM	18.2	42.1	41	64
5/23/2022, 4:00:26 PM	18.2	42.1	40	64
5/23/2022, 4:00:36 PM	18.1	42.2	40	64
5/23/2022, 4:00:46 PM	18.1	42.2	39	64
5/23/2022, 4:00:56 PM	18.1	42.3	38	63
5/23/2022, 4:01:06 PM	18.1	42.3	38	63
5/23/2022, 4:01:16 PM	18.1	42.3	37	62
5/23/2022, 4:01:26 PM	18.1	42.4	36	62
5/23/2022, 4:01:36 PM	18.1	42.4	36	61
5/23/2022, 4:01:46 PM	18.1	42.4	35	61
5/23/2022, 4:01:56 PM	18.1	42.4	35	60
5/23/2022, 4:02:06 PM	18.1	42.5	34	59
5/23/2022, 4:02:16 PM	18.1	42.5	34	59
5/23/2022, 4:02:26 PM	18.1	42.5	33	58
5/23/2022, 4:02:36 PM	18.1	42.6	33	57
5/23/2022, 4:02:46 PM	18.1	42.6	33	57
5/23/2022, 4:02:56 PM	18.1	42.6	32	56
5/23/2022, 4:03:06 PM	18.1	42.7	32	55
5/23/2022, 4:03:16 PM	18.1	42.7	32	55
5/23/2022, 4:03:26 PM	18.1	42.7	31	54
5/23/2022, 4:03:36 PM	18	42.8	31	54
5/23/2022, 4:03:46 PM	18	42.8	31	53
5/23/2022, 4:03:56 PM	18	42.8	31	52
5/23/2022, 4:04:06 PM	18	42.8	30	52

5/23/2022, 4:04:16 PM	18	42.9	30	51
5/23/2022, 4:04:26 PM	18	42.9	30	51
5/23/2022, 4:04:36 PM	18	42.9	30	50
5/23/2022, 4:04:46 PM	18	43	30	50
5/23/2022, 4:04:56 PM	18	43	30	49
5/23/2022, 4:05:06 PM	18	43	30	49
5/23/2022, 4:05:16 PM	18	43	30	48
5/23/2022, 4:05:26 PM	18	43.1	30	48
5/23/2022, 4:05:36 PM	18	43.1	30	47
5/23/2022, 4:05:46 PM	18	43.1	30	47
5/23/2022, 4:05:56 PM	18	43.2	30	46
5/23/2022, 4:06:06 PM	18	43.2	29	45
5/23/2022, 4:06:16 PM	18	43.2	27	45
5/23/2022, 4:06:26 PM	18	43.3	25	44
5/23/2022, 4:06:36 PM	18	43.3	24	44
5/23/2022, 4:06:46 PM	18	43.3	22	44
5/23/2022, 4:06:56 PM	17.9	43.3	21	44
5/23/2022, 4:07:06 PM	17.9	43.4	20	44
5/23/2022, 4:07:16 PM	17.9	43.4	19	44
5/23/2022, 4:07:26 PM	17.9	43.4	18	43
5/23/2022, 4:07:36 PM	17.9	43.4	17	43
5/23/2022, 4:07:46 PM	17.9	43.5	16	41
5/23/2022, 4:07:56 PM	17.9	43.5	16	40
5/23/2022, 4:08:06 PM	17.9	43.6	16	38
5/23/2022, 4:08:16 PM	17.9	43.6	16	37
5/23/2022, 4:08:26 PM	17.9	43.6	16	35
5/23/2022, 4:08:36 PM	17.9	43.6	16	33
5/23/2022, 4:08:46 PM	17.9	43.7	16	32
5/23/2022, 4:08:56 PM	17.9	43.7	16	30
5/23/2022, 4:09:06 PM	17.9	43.7	17	29
5/23/2022, 4:09:16 PM	17.9	43.7	17	28
5/23/2022, 4:09:26 PM	17.9	43.8	17	27
5/23/2022, 4:09:36 PM	17.9	43.8	18	26
5/23/2022, 4:09:46 PM	17.9	43.8	18	26
5/23/2022, 4:09:56 PM	17.9	43.8	19	25
5/23/2022, 4:10:06 PM	17.9	43.9	20	25
5/23/2022, 4:10:16 PM	17.8	43.9	20	25
5/23/2022, 4:10:26 PM	17.8	43.9	21	24
5/23/2022, 4:10:36 PM	17.8	43.9	21	25
5/23/2022, 4:10:46 PM	17.8	43.9	22	25
5/23/2022, 4:10:56 PM	17.8	44	22	25

5/23/2022, 4:11:06 PM	17.8	44	23	25
5/23/2022, 4:11:16 PM	17.8	44	23	26
5/23/2022, 4:11:26 PM	17.8	44	24	26
5/23/2022, 4:11:36 PM	17.8	44	24	27
5/23/2022, 4:11:46 PM	17.8	44.1	24	27
5/23/2022, 4:11:56 PM	17.8	44.1	25	28
5/23/2022, 4:12:06 PM	17.8	44.2	25	29
5/23/2022, 4:12:16 PM	17.8	44.2	25	29
5/23/2022, 4:12:26 PM	17.8	44.2	26	30
5/23/2022, 4:12:36 PM	17.8	44.2	26	31
5/23/2022, 4:12:46 PM	17.8	44.3	26	31
5/23/2022, 4:12:56 PM	17.8	44.3	26	32
5/23/2022, 4:13:06 PM	17.8	44.3	27	32
5/23/2022, 4:13:16 PM	17.8	44.3	27	33
5/23/2022, 4:13:26 PM	17.7	44.4	27	34
5/23/2022, 4:13:36 PM	17.7	44.4	27	34
5/23/2022, 4:13:46 PM	17.7	44.4	27	35
5/23/2022, 4:13:56 PM	17.7	44.4	27	35
5/23/2022, 4:14:06 PM	17.7	44.5	27	36
5/23/2022, 4:14:16 PM	17.7	44.5	27	36
5/23/2022, 4:14:26 PM	17.7	44.5	27	36
5/23/2022, 4:14:36 PM	17.7	44.5	27	37
5/23/2022, 4:14:46 PM	17.7	44.5	27	37
5/23/2022, 4:14:56 PM	17.7	44.6	27	37
5/23/2022, 4:15:06 PM	17.7	44.6	27	38
5/23/2022, 4:15:16 PM	17.7	44.6	27	38
5/23/2022, 4:15:26 PM	17.7	44.6	27	38
5/23/2022, 4:15:36 PM	17.7	44.7	27	38
5/23/2022, 4:15:46 PM	17.7	44.6	27	38
5/23/2022, 4:15:56 PM	17.7	44.7	27	38
5/23/2022, 4:16:06 PM	17.7	44.7	27	39
5/23/2022, 4:16:16 PM	17.6	44.7	27	39
5/23/2022, 4:16:26 PM	17.6	44.8	27	39
5/23/2022, 4:16:36 PM	17.6	44.8	27	39
5/23/2022, 4:16:46 PM	17.6	44.8	27	39
5/23/2022, 4:16:56 PM	17.6	44.8	27	39
5/23/2022, 4:17:06 PM	17.6	44.8	27	39
5/23/2022, 4:17:16 PM	17.6	44.9	27	39
5/23/2022, 4:17:26 PM	17.6	44.9	27	39
5/23/2022, 4:17:36 PM	17.6	44.9	27	39
5/23/2022, 4:17:46 PM	17.6	44.9	27	39

5/23/2022, 4:17:56 PM	17.6	44.9	27	39
5/23/2022, 4:18:06 PM	17.6	44.9	27	39
5/23/2022, 4:18:16 PM	17.6	45	26	39
5/23/2022, 4:18:26 PM	17.6	45	26	39
5/23/2022, 4:18:36 PM	17.5	45	25	39
5/23/2022, 4:18:46 PM	17.5	45	25	39
5/23/2022, 4:18:56 PM	17.5	45	24	39
5/23/2022, 4:19:06 PM	17.5	45	23	39
5/23/2022, 4:19:16 PM	17.5	45	22	39
5/23/2022, 4:19:26 PM	17.5	45	22	39
5/23/2022, 4:19:36 PM	17.5	45.1	21	39
5/23/2022, 4:19:46 PM	17.5	45.1	20	38
5/23/2022, 4:19:56 PM	17.5	45.1	19	38
5/23/2022, 4:20:06 PM	17.5	45.1	18	38
5/23/2022, 4:20:16 PM	17.5	45.1	17	38
5/23/2022, 4:20:26 PM	17.5	45.2	16	38
5/23/2022, 4:20:36 PM	17.5	45.2	15	37
5/23/2022, 4:20:46 PM	17.5	45.2	14	37
5/23/2022, 4:20:56 PM	17.4	45.2	13	36
5/23/2022, 4:21:06 PM	17.4	45.2	12	35
5/23/2022, 4:21:16 PM	17.4	45.2	12	34
5/23/2022, 4:21:26 PM	17.4	45.2	11	34
5/23/2022, 4:21:36 PM	17.4	45.3	10	33
5/23/2022, 4:21:46 PM	17.4	45.3	10	32
5/23/2022, 4:21:56 PM	17.4	45.3	9	31
5/23/2022, 4:22:06 PM	17.4	45.3	8	29
5/23/2022, 4:22:16 PM	17.4	45.3	8	28
5/23/2022, 4:22:26 PM	17.4	45.3	7	27
5/23/2022, 4:22:36 PM	17.4	45.3	7	26
5/23/2022, 4:22:46 PM	17.4	45.3	7	25
5/23/2022, 4:22:56 PM	17.4	45.3	6	23
5/23/2022, 4:23:06 PM	17.4	45.3	6	22
5/23/2022, 4:23:16 PM	17.4	45.3	6	21
5/23/2022, 4:23:26 PM	17.4	45.3	5	20
5/23/2022, 4:23:36 PM	17.3	45.3	5	19
5/23/2022, 4:23:46 PM	17.3	45.3	5	18
5/23/2022, 4:23:56 PM	17.3	45.2	5	17
5/23/2022, 4:24:06 PM	17.3	45.2	5	16
5/23/2022, 4:24:16 PM	17.3	45.2	4	15
5/23/2022, 4:24:26 PM	17.3	45.2	4	15
5/23/2022, 4:24:36 PM	17.3	45.2	4	14

5/23/2022, 4:24:46 PM	17.3	45.1	4	13
5/23/2022, 4:24:56 PM	17.3	45.1	4	12
5/23/2022, 4:25:06 PM	17.3	45.1	3	12
5/23/2022, 4:25:16 PM	17.3	45.1	3	11
5/23/2022, 4:25:26 PM	17.3	45	3	11
5/23/2022, 4:25:36 PM	17.3	45	3	10
5/23/2022, 4:25:46 PM	17.3	45	3	10
5/23/2022, 4:25:56 PM	17.3	45	3	9
5/23/2022, 4:26:06 PM	17.3	44.9	3	9
5/23/2022, 4:26:16 PM	17.3	44.9	3	8
5/23/2022, 4:26:26 PM	17.3	44.9	3	8
5/23/2022, 4:26:36 PM	17.3	44.9	3	8
5/23/2022, 4:26:46 PM	17.3	44.9	2	7
5/23/2022, 4:26:56 PM	17.2	44.9	2	7
5/23/2022, 4:27:06 PM	17.2	44.8	2	7
5/23/2022, 4:27:16 PM	17.2	44.8	2	6
5/23/2022, 4:27:26 PM	17.2	44.8	2	6
5/23/2022, 4:27:36 PM	17.2	44.8	2	6
5/23/2022, 4:27:46 PM	17.2	44.8	2	6
5/23/2022, 4:27:56 PM	17.2	44.8	2	6
5/23/2022, 4:28:06 PM	17.2	44.8	2	5
5/23/2022, 4:28:16 PM	17.2	44.7	2	5
5/23/2022, 4:28:26 PM	17.2	44.7	2	5
5/23/2022, 4:28:36 PM	17.2	44.7	2	5
5/23/2022, 4:28:46 PM	17.2	44.7	2	5
5/23/2022, 4:28:56 PM	17.2	44.7	2	5
5/23/2022, 4:29:06 PM	17.2	44.6	2	4
5/23/2022, 4:29:16 PM	17.2	44.6	2	4
5/23/2022, 4:29:26 PM	17.2	44.6	2	4
5/23/2022, 4:29:36 PM	17.2	44.6	2	4
5/23/2022, 4:29:46 PM	17.2	44.5	2	4
5/23/2022, 4:29:56 PM	17.2	44.5	2	4
5/23/2022, 4:30:06 PM	17.2	44.5	1	4
5/23/2022, 4:30:16 PM	17.2	44.5	1	4
5/23/2022, 4:30:26 PM	17.2	44.5	1	3
5/23/2022, 4:30:36 PM	17.2	44.5	1	3
5/23/2022, 4:30:46 PM	17.2	44.4	1	3
5/23/2022, 4:30:56 PM	17.2	44.4	1	3
5/23/2022, 4:31:06 PM	17.2	44.4	1	3
5/23/2022, 4:31:16 PM	17.2	44.4	1	3
5/23/2022, 4:31:26 PM	17.2	44.4	1	3

5/23/2022, 4:31:36 PM	17.2	44.3	1	3
5/23/2022, 4:31:46 PM	17.2	44.3	1	3
5/23/2022, 4:31:56 PM	17.2	44.3	1	3
5/23/2022, 4:32:06 PM	17.1	44.3	1	3
5/23/2022, 4:32:16 PM	17.1	44.3	1	3
5/23/2022, 4:32:26 PM	17.1	44.3	1	3
5/23/2022, 4:32:36 PM	17.1	44.3	1	3
5/23/2022, 4:32:46 PM	17.1	44.2	1	3
5/23/2022, 4:32:56 PM	17.1	44.2	1	2
5/23/2022, 4:33:06 PM	17.1	44.2	1	2
5/23/2022, 4:33:16 PM	17.1	44.2	1	2
5/23/2022, 4:33:26 PM	17.1	44.2	1	2
5/23/2022, 4:33:36 PM	17.1	44.2	1	2
5/23/2022, 4:33:46 PM	17.1	44.2	1	2
5/23/2022, 4:33:56 PM	17.1	44.2	1	2
5/23/2022, 4:34:06 PM	17.1	44.2	1	2
5/23/2022, 4:34:16 PM	17.1	44.1	1	2
5/23/2022, 4:34:26 PM	17.1	44.1	1	2
5/23/2022, 4:34:36 PM	17.1	44.1	1	2
5/23/2022, 4:34:46 PM	17.1	44.1	1	2
5/23/2022, 4:34:56 PM	17.1	44.1	1	2
5/23/2022, 4:35:06 PM	17.1	44.1	1	2
5/23/2022, 4:35:16 PM	17.1	44.1	1	2
5/23/2022, 4:35:26 PM	17.1	44.1	1	2
5/23/2022, 4:35:36 PM	17.1	44.1	1	1
5/23/2022, 4:35:46 PM	17.1	44.1	1	1
5/23/2022, 4:35:56 PM	17.1	44.1	1	1
5/23/2022, 4:36:06 PM	17.1	44.1	1	1
5/23/2022, 4:36:16 PM	17	44.1	1	1
5/23/2022, 4:36:26 PM	17	44.1	1	1
5/23/2022, 4:36:36 PM	17	44.1	1	1
5/23/2022, 4:36:46 PM	17	44.1	1	1
5/23/2022, 4:36:56 PM	17	44.1	1	1
5/23/2022, 4:37:06 PM	17	44.1	1	1
5/23/2022, 4:37:16 PM	17	44.1	1	1
5/23/2022, 4:37:26 PM	17	44.1	1	1
5/23/2022, 4:37:36 PM	17	44.1	1	1
5/23/2022, 4:37:46 PM	17	44.1	1	1
5/23/2022, 4:37:56 PM	17	44.1	1	1
5/23/2022, 4:38:06 PM	17	44.1	1	1
5/23/2022, 4:38:16 PM	17	44.1	1	1

5/23/2022, 4:38:26 PM	17	44.1	1	1
5/23/2022, 4:38:36 PM	17	44.1	1	1
5/23/2022, 4:38:46 PM	17	44.1	1	1
5/23/2022, 4:38:56 PM	17	44.1	1	1
5/23/2022, 4:39:06 PM	17	44.1	1	1
5/23/2022, 4:39:16 PM	17	44.1	1	1
5/23/2022, 4:39:26 PM	17	44.1	1	1
5/23/2022, 4:39:36 PM	17	44.1	1	1

APPENDIX C: ADDITIONAL SEM IMAGES

Below are additional images of the carbon samples taken at higher magnifications using SEM (referenced previously in Section 3.3.3). The magnifications of the images below vary from 20,000X to 50,000X.

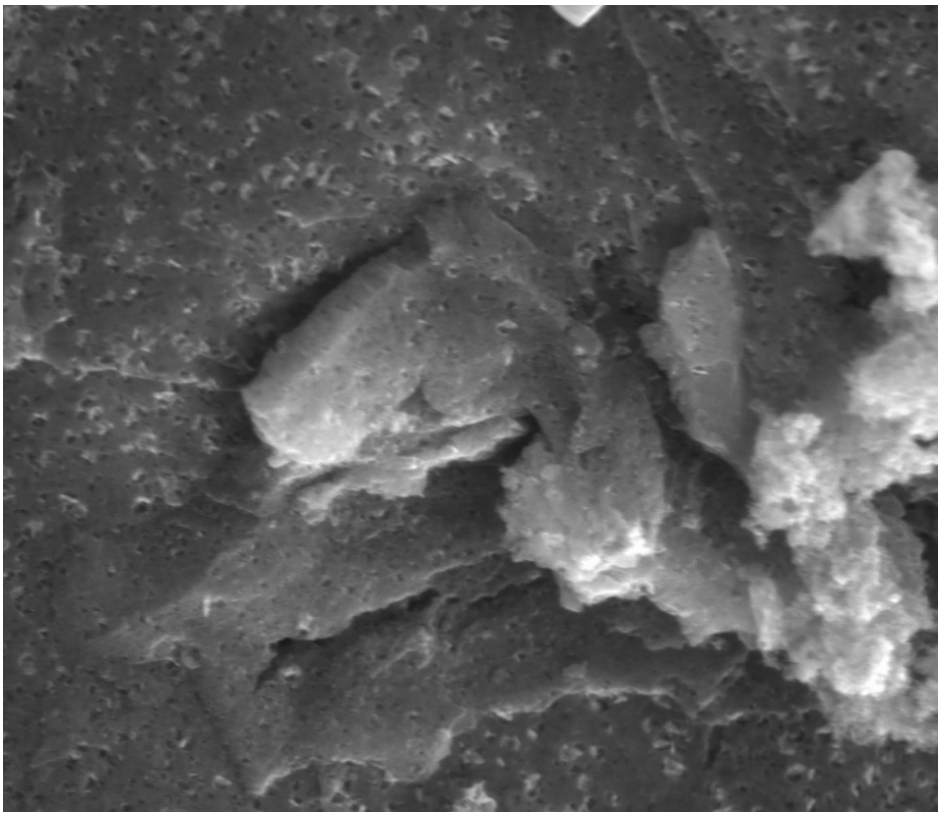

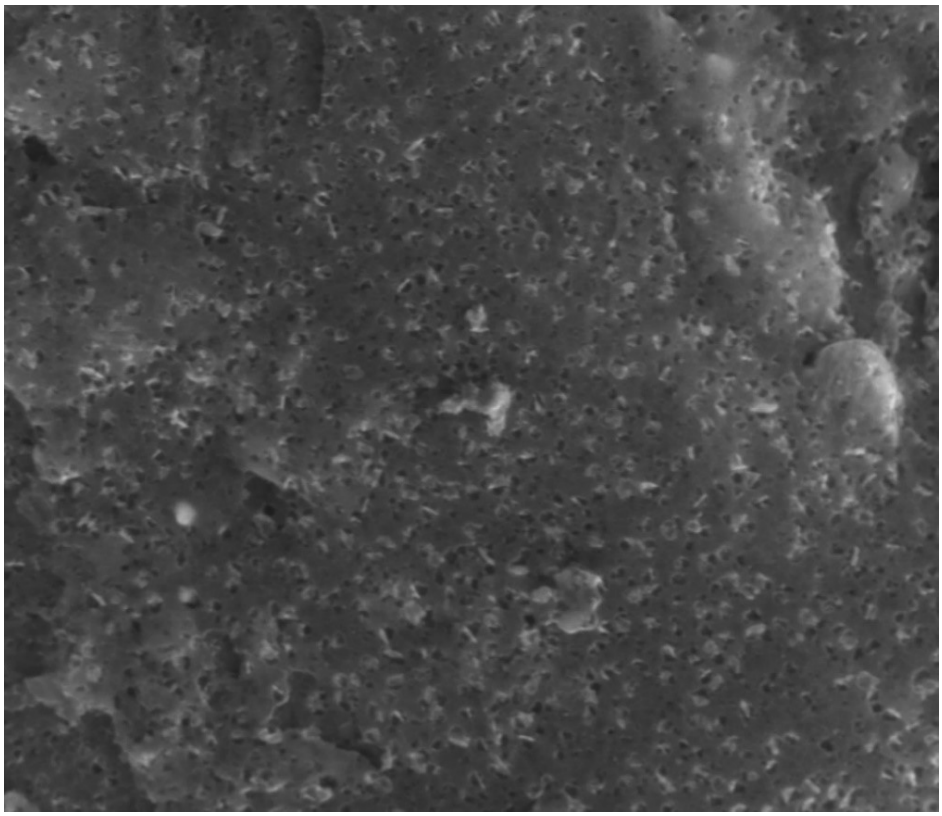

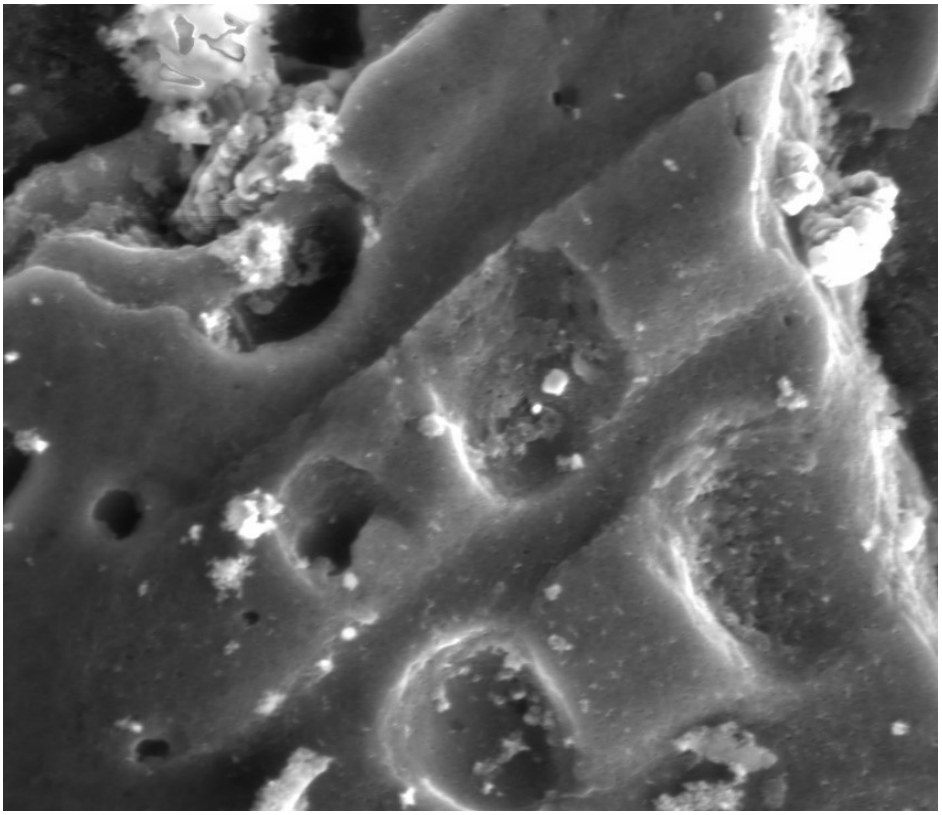

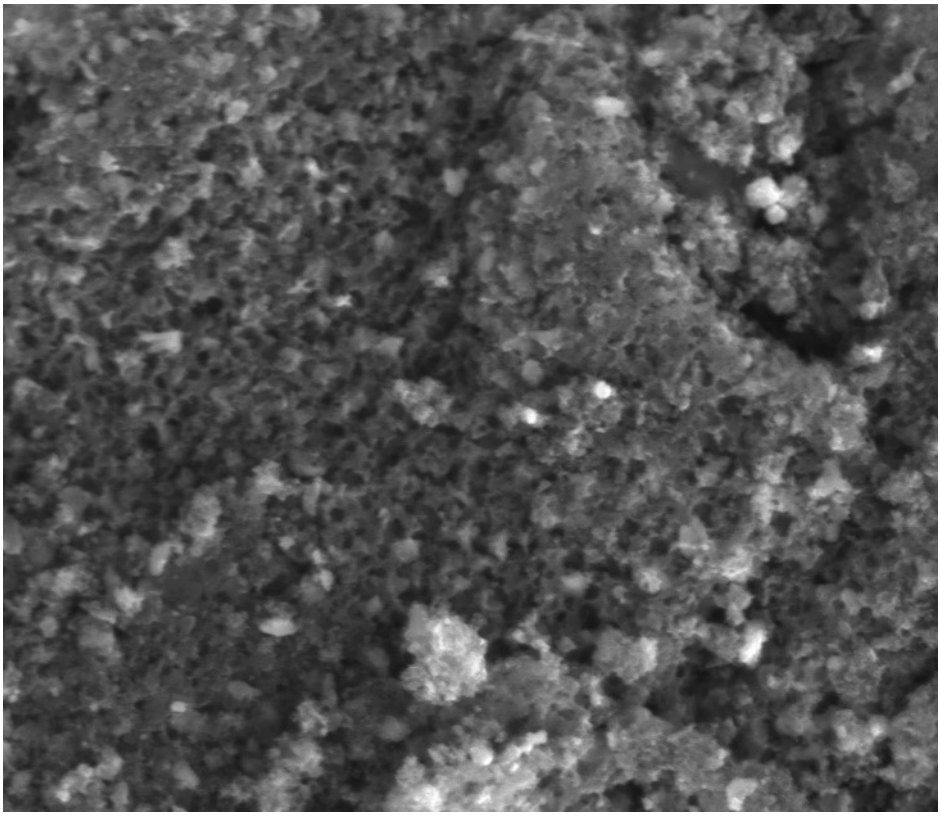

APPENDIX D: POWER CONSUMPTION OF ODOR CONTROL DEVICE

The power consumption of the odor control device was calculated based on a sample period of operation which includes a 15-minute period of H_2S adsorption and a 45-minute period of thermal regeneration/desorption. During the period of adsorption, the regenerative blower is turned on and the air is directed through a column packed with AC without the assistance of any other power-consuming devices. After desorption, the column is heated for half an hour by heat tape and then air is pumped through the column via the air compressor for 15 minutes. The estimated power usage appears below in Table D.1. Over the course of one cycle, the device uses approximately 1 kW-hr, which typically costs about $0.10.

Table D.1: Power Consumption of Odor Control Device

Item	Current Draw (Amps)	Power (W)	Time (Minutes)	Power Use (kW-hr)	Cost
Blower	7.4	888	30	0.444	$0.04
Compressor	6.6	792	15	0.198	$0.02
Heat Tape	2.6	312	45	0.234	$0.02
TOTAL	16.6	1992	90	0.876	$0.09

APPENDIX E: SAMPLE CALCULATIONS

The movement of H_2S through the pilot odor control device was monitored using H_2S sensors. These sensors generated data showing the concentration of H_2S (ppm) in 10-second intervals. The efficiency of adsorption, desorption and BTF treatment was calculated using a mass balance for each experiment. The raw data, concentration of H_2S in ppm, is first converted to mg/L using the ideal gas law (equation below).

$$\mathrm{C}\left(\frac{\mathrm{mg}}{\mathrm{L}}\right) = \mathrm{C(ppm)} * \frac{\mathrm{MW}}{\mathrm{MV}} * \frac{\mathrm{T(°C)} + 273}{273} * \frac{1}{1000}$$

This value is converted to a mass flow rate using the measured volumetric flow rate (L/min) at either the inlet or the outlet. In the instance of the landfill experiments, the flow rate was 0.25 L/min because the gas was supplied to the sampler at this flow rate. This mass flow rate is converted to a cumulative mass using the time step (10 seconds).

APPENDIX F: TROUBLESHOOTING AND OTHER INFORMATION

The following list includes troubleshooting information for various issues encountered during the operation of the pilot device. Additional information regarding design decisions and lessons learned appear in this appendix in hopes of providing a helpful guide to future users of the pilot odor control device and its accompanying equipment.

- The size of the pipes carrying the air to each part of the pilot device was adjusted at various points throughout the design process to reduce losses due to friction. Initially, 1/4” tubing was used with 3-way solenoid valves with 1/4” ports. In the final design, 1” PVC piping was used along with solenoids with 1” ports.
- The solenoids used in the current iteration of the pilot device require a power input that is too large for a standard irrigation controller to provide. For this reason, it received additional current from a transformer via relays that are wired together according to the wiring diagram that appears in Appendix A (Figure A.2). When one pair of solenoid valves was turned on, the flow of air was changed from one GAC column to the other. This would allow for two columns to be used interchangeably. The operation of the solenoid valves was displayed previously in Figure 5.6.
- In colder temperatures, it is important to consider the tubing which carries the nutrient solution to the BTF. When water freezes inside the nutrient solution line, it will often burst. Some steps that were taken to prevent this phenomenon from happening included:

    - Installing insulation around tubing, the bucket that contained the nutrient solution, and the fluid metering pump.
    - Installing a heated pad underneath the bucket containing the nutrient solution.
    - Installing a heated cord around the BTF.
    - Implementing an "air purge" that occurred after nutrient solution was pumped to the BTF. Air was pumped through the tubing following the trickling fluid to remove any water from the line.
- The sensors used to measure H_2S at various locations in the system should be kept in the sampling system (yellow box) when possible, as they are sensitive to moisture in the air and can be damaged if exposed to high temperatures; the recommended temperature range for these sensors is -20 to 50°C. The sampling system provides a protective barrier between both moisture and excessive heat.
- Always make sure to turn the H_2S sensors to "logging" mode by holding the button on top of each sensor before beginning data collection.
- During heating of the GAC columns, it is important to carefully observe the temperature of the columns. It was determined that virgin carbon used in experimentation can emit SO_2, which will produce inaccurate results. In contrast, the steel columns did not produce sulfur oxides. Nonetheless, it is recommended that regular measurements with a temperature gun are taken of the column at or near where the heat tape is placed to ensure that:
    - The carbon reaches the desired temperature.

  - An exothermic reaction is not occurring, which would produce emissions of sulfur in quantities that would obscure the data.

- Heat emitted by the GAC columns was monitored to prevent damage to other components of the pilot device. Some measures taken to reduce the effects of the emitted heat include:
  - Selecting stainless steel piping to transport gas from the GAC columns to the BTF.
  - Wrapping the GAC columns in insulation to prevent the conduction of heat to the structural components of the system.
  - Applying a heat sink compound to the top and bottom of the column to minimize heat transfer.
- To allow the device to run autonomously, two boxes that contain timers were programmed to turn on each component of the pilot device at specified times. During experimentation, the device required the addition of H_2S for data collection which prevented remote operation. Thus, the pilot device was never run autonomously, except for the pumping of the trickling fluid into the BTF. In future experiments, the use of the timer boxes would provide for simple treatment of H_2S if remote operation is possible.